THERMO-RESPONSIVE LAYER-BY-LAYER ASSEMBLIES FOR NANOPARTICLE-BASED DRUG DELIVERY

A Thesis

by

JING ZHOU

Submitted to the Office of Graduate and Professional Studies of
Texas A&M University
in partial fulfillment of the requirements for the degree of

MASTER OF SCIENCE

Chair of Committee, Michael Pishko
Co-Chair of Committee, Jodie Lutkenhaus
Committee Member, Zhengdong Cheng
Head of Department, Ibrahim Karaman

December 2013

Major Subject: Materials Science and Engineering

ABSTRACT

Layer-by-layer (LbL) capsules, known for their versatility and smart response to environmental stimuli, have attracted great interest in drug delivery applications. However, achieving a desired drug delivery system with sustained and tunable drug release in response to temperature is still challenging. Here, a thermo-responsive drug delivery system of solid dexamethasone nanoparticles (DXM NPs) encapsulated in a model LbL assembly of strong polyelectrolytes poly (diallyldimethylammonium chloride)/poly (styrene sulfonate) (PDAC/PSS) was constructed.

DXM NPs at an average size of 201 ± 96 nm were fabricated. ζ-potential measurements, X-ray photoelectron spectroscopy, and transmission electron microscopy confirmed the successful adsorption of each layer. The influence of various parameters on drug release, such as number of layers, ionic strength of the adsorption solution, temperature and outer-most layer, has been investigated. Results have shown a controlled DXM release from LbL nanoshells by tuning number of layers and ionic strength of the adsorption solution. The DXM release from linearly growing LbL of PDAC/PSS (assembled without NaCl), which do not exhibit a glass transition, experienced a more temperature response than those from exponentially growing LbL of PDAC/PSS (assembled at 0.5 M NaCl), which exhibit a glass transition. Such a difference was attributed to be related with the free volume cavities within the assemblies. By tailoring the properties of those cavities, an ideal thermo-responsive drug delivery system may be obtained. This thermo-responsive NP-based drug delivery

system with tunable permeability may possibly realize an “on” or “off” drug release mechanism in response to temperature, thus providing an alternative approach to delivery therapeutics with reduced toxic effects.

ACKNOWLEDGEMENTS

I am grateful to my advisors, Dr. Pishko, Dr. Lutkenhaus, and my committee member Dr. Cheng, for their guidance and support throughout the course of this research. They not only taught me how to do research, but also helped me a lot in life. Their attitude toward research, and their personalities always inspired me.

I would also like to thank Joan and Matt from National Center for Therapeutics Biomanufacturing (NCTM) for helping me set up equipment. Without their help, I could not have finished my degree so smoothly. Thanks also extend to the staff of the Materials Characterization Facility (MCF) for technical training. Thanks to my group members for a lot of discussion, especially Minchi-Hsieh, Choonghyun Sung and Xiayun Huang.

Finally, thanks to my grandma and my parents for their strong support.

TABLE OF CONTENTS

Page

LIST OF FIGURES

LIST OF TABLES

1. INTRODUCTION

1.1 Motivation and Hypothesis

Cancer, known as a broad group of diseases involving unregulated cell growth, is the leading cause of death worldwide. The transformation of a normal cell into a cancer cell is identified with the alteration of genes regulating cell growth and differentiation.[1] The search for the origin and treatment of cancer remains a grand challenge.[2]

To date, effective cancer treatments include chemotherapy, surgery, radiation, and immunotherapy. Recently, combination therapy under remote physical controls has received great attention as a new theranostic approach to decrease systemic toxicity, and avoid overdosing. External stimuli, including light, magnetic field, electric field, and heat, have been used to trigger, control, and enhance localized cancer therapies.[2] Because heat can be utilized to directly destroy cancer cells, the delivery of anti-cancer drug triggered by heat is of special interest for combined cancer treatment.

Layer-by-layer (LbL) capsules, which are nanoscale shells built up through the alternating adsorption of oppositely charged polyelectrolytes on a spherical substrate via electrostatic interactions, have attracted great interest for use as multifunctional therapeutic delivery vehicles.[3,4, 5,6] The highly versatile LbL assembly technique allows one to engineer the size, shape, permeability, and surface functionality of capsules by simply selecting layer species and assembly conditions, such as ionic strength,[7,8] pH,[9,10] and temperature.[11,12,13] However, a “smart” delivery system, where permeability changes in response to environmental stimuli, still wait to be explored.

Very recently a class of layer-by-layer (LbL) assemblies has been found to exhibit a glass transition at slightly above the body's physiological temperature. For example, Vidyasagar *et al.*[14] in our group found a step increase in viscoelasticity for hydrated exponentially growing LbL assemblies of strong polyelectrolytes poly (diallyldimethylammonium chloride)/poly (styrene sulfonate) (PDAC/PSS) at 49-56 ^{o}C, coinciding with films' glass transition temperature (T_g), Figure 1-1. No distinct transition was observed for linearly growing assemblies at this temperature window. The increase in viscoelasticity was attributed to the breaking of ion pairs and subsequent chain relaxation, reflecting an increase in polymer chain mobility. As suggested by Johansson,[15] solute diffusion increases as polymer chains become more flexible, providing evidence that polymer chain mobility is an important governing factor. Ion transport through polymers such as poly (ethylene oxide) typically jumps at temperatures around the T_g.[16] Thus we hypothesize that the distinct glass transition observed in exponentially growing PDAC/PSS LbL assemblies may cause an enhancement in drug permeability, which motivated us to develop a thermo-responsive drug delivery system by assembling PDAC/PSS onto solid drug nanoparticles to form a core-shell structure. If such a hypothesis is true, one might expect a greater response to temperature for the release of drug from exponentially growing PDAC/PSS nanoshells as compared to drug release from linearly growing PDAC/PSS nanoshells.

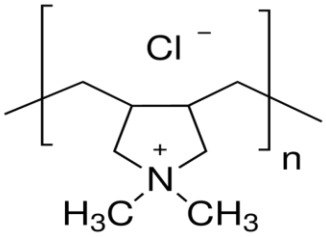

Poly (diallyldimethylammonium chloride) (PDAC)

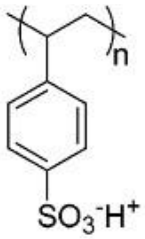

Poly (styrene sulfonate) (PSS)

Figure 1-1. Chemical structures of PDAC and PSS; reproduced from 17,18.

Dexamethasone, a synthetic gluococorticoid that suppresses inflammation and autoimmune conditions, is given to cancer patients undergoing chemotherapy to reduce nausea and other side effects of cancer treatment, [19, 20] Figure 1-2. Dexamethasone is partly water-soluble; the solubility in PBS is about 140 μg/ml. [21] However, dexamethasone can cause serious systemic side effects including hypertension, psychiatric disturbances and diabetes mellitus. To avoid these side effects, a controlled and continuous delivery of dexamethasone is desired.

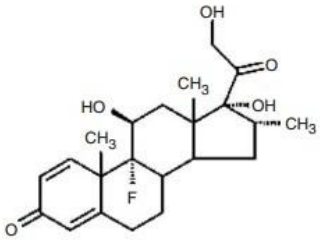

Figure 1-2. Chemical structure of dexamethasone; reproduced from 22.

In this present study, a thermo-responsive drug delivery system of solid dexamethasone nanoparticles (DXM NPs) encapsulated in a model layer-by-layer (LbL) assembly of strong polyelectrolytes poly (diallyldimethylammonium chloride)/poly (styrene sulfonate) (PDAC/PSS) will be constructed. Specifically, the effect of temperature on DXM release will be investigated.

1.2 Specific Aims

1.2.1 Fabrication and LbL encapsulation of dexamethasone based core-shell structured nanoparticles

This thermo-responsive drug delivery system consists of a dexamethasone based core encapsulated by LbL assemblies of strong polyelectrolytes PDAC/PSS, Figure 1-3. The solid dexamethasone drug nanoparticles will be fabricated by a modified emulsion solvent evaporation technique and then encapsulated into PDAC/PSS synthetic polymers through a layer-by-layer assembly technique.

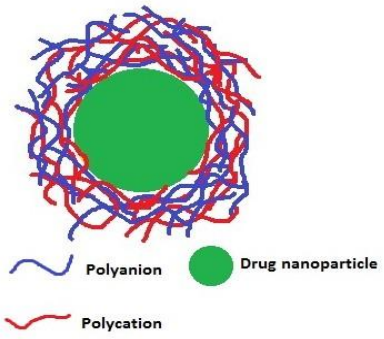

Figure 1-3. PDAC/PSS layer pairs assembled on drug nanoparticles

1.2.2 *In vitro* dexamethasone release studies

The dexamethasone release from PDAC/PSS LbL shells will be determined by measuring drug concentration versus time. It was observed[18] that there was a glass transition at 49-56 ^{o}C for PDAC/PSS LbL assembled at 0.5 M NaCl, while no glass transition was observed for those assembled without NaCl. Thus the PDAC and PSS LbL shells will be assembled at 0.5 M NaCl and no NaCl respectively and release experiments will be conducted at 37 ^{o}C and 60 ^{o}C. The effect of varying (i) number of layers, (ii) ionic strength of the adsorption solutions, (iii) temperature, and (iv) outer-most layer on dexamethasone release will be examined.

2. LITERATURE REVIEW

2.1 Introduction

This present chapter introduces the development of nanoparticle-based drug delivery system for cancer treatment, applications of layer-by-layer capsules in drug delivery, factors affecting the permeability of LbL assemblies, and existing examples of thermo-responsive layer-by-layer capsules. This chapter gives an insight into the interplay of physiochemical parameters and LbL properties, providing a guide in the design of thermo-responsive drug delivery vehicles.

2.2 Nanoparticle-Based Drug Delivery Systems

Drug delivery systems are designed to improve the therapeutic properties of conventional ("free") drugs, where free drugs are primarily encapsulated within, or attached to, lipids or polymers. Examples of problems associated with free drugs include poor drug solubility, loss of activity *in vivo*, unfavorable pharmacokinetics, and poor biodistribution.[23] Efficient drug delivery systems allows for precisely controlled pharmacokinetics and preferentially localized sites of delivery to reduce systemic side effects and dosages required.[24,25]

With the emergence of nanotechnology, nanoparticle-based therapeutics has significant potential to revolutionize medical treatment with more potent and less toxic delivery systems.[26, 27] With substantial efforts devoted into this field, a few nanoparticle-based formulations, such as protein-based nanoparticles (NPs) (Abraxane®, Celgene

Corporation), lipid-based NPs (Inflexal® V, Crucell), and polymer-based NPs (ELIGARD®, Sanofi), have been approved by the FDA for clinical use. One important advantage of NPs as drug delivery systems is targeting because their small size can efficiently penetrate across biological barriers.[28] Intravenously administered therapeutics circulates in the bloodstream and interacts with the reticuloendothelial system (RES), a part of the immune system to clear foreign entities, prior to arriving at the target site. The efficiency of NPs to target at the site of diseases is dependent on a number of factors including size, shape, and surface chemistry.[29] For tumor targeting, particles less than 250 nm are preferred because they are more likely to cross the extravasation (leaky endothelium of tumor). The shape of particles is known to affect the flowing directions in which particles flow through a vessel. Because particles interact with various components of the blood while flowing through the vessel, surface functionality of particles is an effective strategy to prevent particles being cleared by the RES and hence prolong the circulation time. For example, particles functionalized with hydrophilic polymers such as polyethylene glycol (PEG) have been shown to prolong the circulation time by minimizing their interactions with the RES. [29]

Numerous polymer-based delivery systems have been developed to encapsulate therapeutics. As shown in Figure 2-1, the drug is encapsulated into a polymer membrane in a reservoir system; the drug is evenly distributed through a polymer system in a matrix system. By selecting appropriate polymers according to the goal of the drug delivery system, various properties such as formulation, particle size, permeability, and sustained-release properties may be tuned. Despite existing strategies render solutions to

achieve the goal of reducing toxic effects, achieving the desired NP-based drug delivery system with such versatility is still challenging.

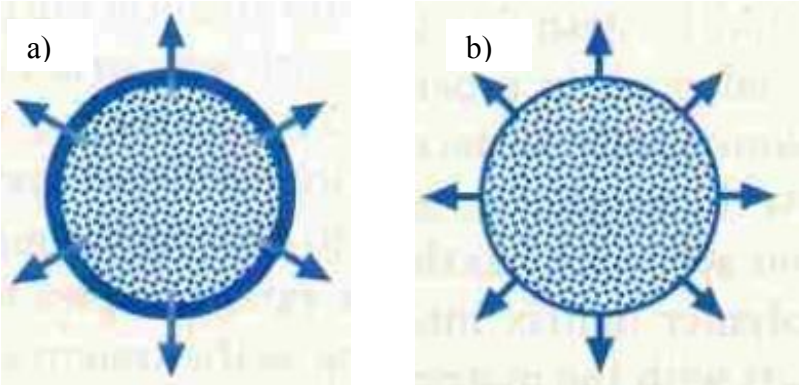

Figure 2-1. Examples of polymer-based delivery system. Small dots represent drug, and arrows show the direction in which drug is released. a) reservoir system, b) matrix system (reproduced from reference 25).

2.3 Layer-by-Layer (LbL) Capsules for Drug Delivery

LbL assembly, pioneered by Decher, is a technique for the construction of nanoscale films by alternate adsorption of polyelectrolytes from aqueous solution.[30] Interactions between polyelectrolytes, including electrostatic, hydrogen bonding, and Van der Waals, have been considered to drive the formation of these nanoscale films, but entropy is the major driving force. Various substrates, such as glass slides, charged particles, carbon nanotubes, and porous membranes, have been used as supports for building these LbL assemblies.

Recently, layer-by-layer (LbL) particles, which are nanoscale shells built up through the alternate adsorption of oppositely charged polyelectrolytes on a spherical

substrate, have attracted great interest for use as multifunctional therapeutic delivery vehicles.[3,4,5,6] These coated LbL particles are considered core-shell particles. By removal of the sacrificial particle core, hollow LbL capsules are formed. Therapeutics including small molecule drugs, peptides, proteins, and growth factors can be loaded into capsules and released at a desired rate. The highly versatile LbL assembly technique allows one to engineer the size, shape, permeability, and surface functionality of capsules by simply selecting layer species and assembly conditions, such as ionic strength,[7,8] pH,[9,10] and temperature.[11,12,13] However, a "smart" delivery system, where the permeability of microcapsules or nanoshells changes in response to environmental stimuli, still waits to be explored. External stimuli including salt,[31] pH, heat,[32,33] and light[34] can induce the permeability changes, Figure 2-2. For example, Möhwald and co-workers prepared hollow capsules of poly (allylamine) (PAH)/PSS. The permeability of the capsule was found to be reversibly switched between an open and a closed state for PAH (70000 g/mol) by changing the adsorption salt concentration from 5 to 20 mM. Tsukruk *et al.* reported the pH-responsive permeability of hydrogen bonded hollow microcapsules of tannic acid assembled with a range of neutral polymers, poly(N-vinylpyrrolidone) (PVPON), poly(N-vinylcaprolactam) (PVCL) or poly(N-isopropylacrylamide) (PNIPAM).[35] These stimuli-responsive phenomena reveal the complex nature of polyelectrolytes and highlight the interplay of parameters which can affect the permeability of microcapsules or nanoshells.[36]

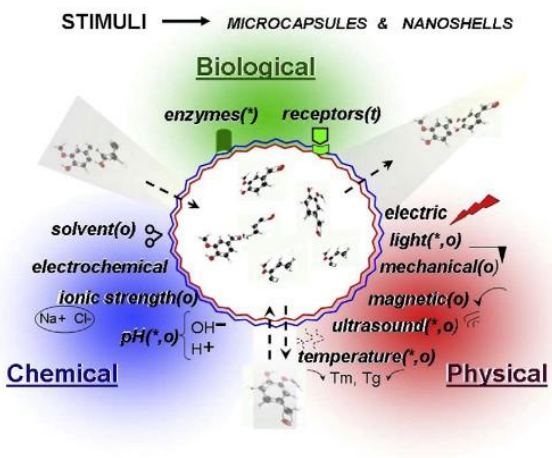

Figure 2-2. Schematic illustration of stimuli for microcapsule loading and release (Reproduced from 36).

2.4 Factors Affecting the Permeability of LbL Assemblies

For drug release, the permeability of capsules is particularly important in order to achieve the proper release profile over a given period of time. Studies on the permeability of LbL assemblies have been reviewed by Mansouri and co-workers.[37] Physicochemical parameters including ionic strength, layer number, and pH have been reported to affect the permeability of LbL assemblies. To investigate the permeability of LbL microcapsules or nanoshells, several methods are indicated in the literature. One method is to add a fluorescent probe solution to the capsules and to monitor the permeation of the probe into capsules by means of confocal laser scanning imaging (CLSM).[31] A second method is to encapsulate a crystalline material within the LbL shells and measure the release of core material into the bulk solution.[38] A more recent approach is by applying a molecular beacon (MB) technique, where MB-functionalized

particles are encapsulated within LbL shells and then incubated with DNA target sequences of different lengths. Permeation of the DNA target causes the hybridization of DNA targets with the complimentary loop regions of the MBs, resulting in an increase in MB fluorescence.[39]

It is well known that the diffusion of solute through the LbL film is likely to take place through water-filled cavities existing in LbL films.[40, 41] Any factor which can alter the size of these spaces, including polymer chain mobility, the size of the solute in relation to the size of the cavities, and the existence of charged groups on the polymer which may bind the solute molecule, will cause a variation in the diffusivity of a solute.[42] Because local defects, or free volume cavities existing in LbL films are crucial for controlled release applications, attempts to probe the nanoscale porosity of LbL films have been reported by several groups. Chavez and Schönhoff estimated the porosity of PAH/PSS LbL shells formed on colloidal particles using NMR cryoporometry, and found that the pore size was ~1 nm.[43] Quinn *et al.* made use of positron annihilation spectroscopy (PAS) technique to measure the Ångström-scale free volume, and investigated the effect on the free element volume size and concentration elements in LbL of varying film assembly conditions.[44] They found that depending on the number of layer pairs and the assembly conditions selected, the diameters of free volume cavities can be tuned from 0.4 to 0.6 nm, and the total free volume concentrations varies from 1.1×10^{20} to 4.3×10^{20} cm^{-3}.[44] Other investigation by Köhler *et al.*,[45] using a permeation approach by encapsulating fluorescent dextran with different molecular weights and quantifying the entrapped amount after release, estimated an apparent mesh size of 13

nm for PSS-terminated PDAC/PSS LbL microcapsules. This value was attributed to the large defects within the PDAC/PSS LbL.

2.5 Thermo-Responsive LbL Capsules

Thermo-responsive LbL assemblies were introduced via several approaches over the past decade. A well-known approach is to introduce thermo-responsive polymers undergoing coil-globular phase transitions into LbL assemblies. When temperature is raised above a low critical solution temperature (LCST), thermo-responsive polymers transition from a collapsed dehydrated state to a swollen state causes an increase/decrease in the permeability depending on LbL assembly conditions. For example, Quinn and Caruso[46] assembled hydrogen bonded LbL films of poly (N-isopropylacrylamide) (PNIPAAm)/poly (acrylic acid) (PAA) and found a temperature-dependent dye loading and release behavior. Such a behavior was attributed to depend on molecular interactions between the probe molecule and PNIPAAm. The addition of a hydrophobic moiety within the assemblies could significantly decrease dye release rate as well as enhance the thermo-responsive performance of films. Sukhishvili *et al.*[47] incorporated triblock copolymers poly(N,N-dimethylaminoethyl methacrylate)-b-poly(propylene oxide)-b-poly(N,N-dimethylaminoethyl methacrylate) (PD-PPO-PD) into LbL assemblies. Because the dehydration temperature of the central PPO block was strongly dependent on pH, a dual pH and temperature-responsive reversible swelling and deswelling properties was observed. Wang *et al.*[48] assembled PNIPAAm/alginate acid on $MnCO_3$ cores and obtained microcapsules after removal of the templates. Thermo-

sensitivity due to the conformation change of PNIPAAm, and pH-sensitivity due to the cross linking of Mn^{2+} were observed in such microcapsules.

It has been considered that factors, such as the presence of excess charge or the intermolecular association of polymer units, affect polymers temperature responsiveness.[49] The presence of extra charge within LbL films was shown to suppress the temperature-responsiveness of films via enhanced film swelling.[50] An increased complexation of hydrogen bonded multilayers of poly(methacrylic acid) (PMAA)/poly(N-vinylcaprolactam) (PVCL) and PMAA/poly(vinyl methylether) (PVME) with poly(carboxylic acids) was shown to suppress thermo-responsive properties, indicating that the strength of intermolecular interaction plays an important role in polymers temperature responsiveness.[33]

Glass transition corresponding to a change in mobility/viscoelasticity is also known to affect films permeability. Lin *et al.*[51] discovered that the water vapor permeability to poly(ethylene oxide glycol)/polybutyleneadipate multiple-polyol system of polyurethane films increases dramatically at temperatures near the films' glass transition temperature(T_g). Other than these advances, very little is known about the permeability of LbL films in response to the glass transition.

As shown by Vidyasagar *et al.*[14] in our group, a glass transition was observed for for hydrated exponentially growing LbL assemblies of strong polyelectrolytes PDAC/PSS. In this present thesis, PDAC/PSS LbL assemblies will be coated onto drug nanoparticles. Several remarkable works on the thermal behavior of PDAC/PSS LbL microcapsules have been done. Mueller *et al.*[52] reported that PDAC/PSS LbL capsules

experienced a melting process from glassy to viscoelastic state at 35-40 ^{o}C, where the Young's modulus decreases significantly as measured by means of Atomic Force Microscopy (AFM). This was attributed to the breakage of ionic bonds, allowing the rearrangement of oppositely charged polyelectrolytes to occur. Köhler *et al.*[53] observed an "odd-even" effect on PDAC/PSS LbL capsules, where PSS-terminated capsules shrank at 35-40 ^{o}C upon heating and PDAC-terminated ones swelled, as determined by CLSM and scanning electron microscopy (SEM). Ghostine and Schlenoff[54] reported that the diffusion coefficient of ferricyanide probing ions through PSS–terminated PDAC/PSS LbL films increased strongly upon heating (14-50 ^{o}C); however, no clear phase transition was observed.

3. MATERIALS AND METHODS

3.1 Introduction

This chapter presents the materials and methods used in this study. Dexamethasone nanoparticles (DXM NPs) were fabricated by a two organic solvent evaporation technique. LbL assemblies were coated onto DXM NPs from different assembly conditions. ζ -potential measurements, X-ray photoelectron spectroscopy (XPS), and transmission electron microscopy (TEM) were used to confirm the success of layer adsorption. *In vitro* release studies of dexamethasone from PDAC/PSS LbL NPs were carried out at 37 ^{o}C and 60 ^{o}C. The concentration of released dexamethasone was assayed by high performance liquid chromatography (HPLC).

3.2 Materials

Poly (diallyldimethylammonium chloride) (PDAC, Mw~350 000 g/mol) and poly (styrene sulfonate sodium salt), (PSS, Mw~500 000 g/mol) were purchased from Sigma Chemicals and Scientific Polymer Products respectively. USP grade dexamethasone was obtained from Sigma Chemicals. Acetone and n-Heptane were purchased from Sigma Chemicals, USA, and Acros Organics respectively. HPLC grade acetonitrile and water were purchased from Avantor Materials. Ultrapure water used for all experiments was obtained from a Pall Corporation Cascada^{TM} LS-water purification system with a specific resistance of 18.2 MΩ/cm. Phosphate-buffered saline solution (PBS, pH=7.4) consisted of 1.1 mM potassium phosphate monobasic, 3 mM sodium

phosphate dibasic heptahydrate, and 0.15 M sodium chloride. VWR syringe filters of size 0.2 μm were purchased from VWR and BD syringes were purchased from BD. A Fisher Scientific Marathon 16KM Centrifuge and an Eppendorf Centrifuge 5804 were used for the centrifugation procedures.

3.3 Preparation of DXM NPs

DXM NPs were prepared by a modified solvent evaporation technique described elsewhere.[55, 56, 57] In this technique, immiscible liquids form droplets of drug, which are hardened by solvent evaporation to form micro or nano particles.[58] Here, a solution of dexamethasone in acetone (0.5%w/v) was mixed into n-Heptane with a v/v ratio of 2 to 1 at 50 ^{o}C for 30 min. To ensure that n-Heptane was completely removed, DXM NPs were resuspended in PBS and constantly stirred overnight at room temperature. All nanoparticles were stored in a refrigerator until future use. The encapsulation efficiency (E.E.) of DXM NPs was calculated as the mass ratio of DXM mass encapsulated and the initial DXM mass. To measure the DXM mass encapsulated, 10 μl of DXM NPs from the stock solution were dissolved in 1 mL acetonitrile and its concentration was determined by HPLC analysis described later.

$$\text{DXM NPs E.E. \%} = \frac{\text{Mass of DXM encapsulated in NPs}}{\text{Mass of DXM initially fed}} \times 100\% \qquad 3\text{-}1$$

3.4 Layer-by-Layer Assembly on DXM NPs

20 mg/ml solutions of PDAC and PSS were prepared from their respective homopolymers and ultrapure water with ionic strengths of 0 or 0.5 M NaCl at pH 7.4. LbL NPs were constructed by the alternate adsorption of polyelectrolytes onto negatively charged DXM NPs until a desired layer number was obtained. Polyelectrolyte solutions were incubated with 10~20 mg/ml DXM NPs for 20 min followed by centrifugation and removal of supernatant. Three separate rinses with respective ionic strength were performed between each layer adsorption, Figure 3-1.

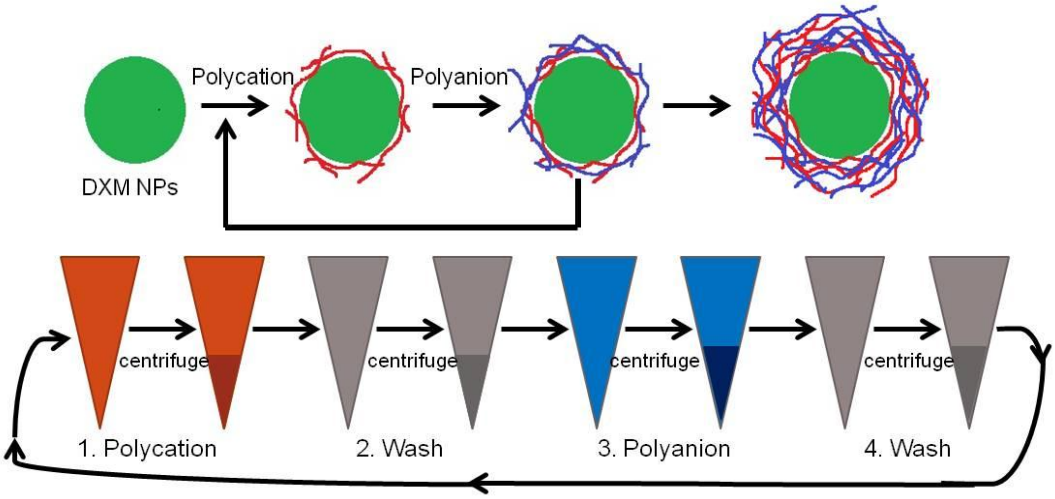

Figure 3-1. The procedure of LbL coating on DXM NPs

3.5 *In Vitro* DXM Release from LbL Assemblies

Release studies of dexamethasone from PDAC/PSS LbL NPs were performed *in vitro*. 1.0 mL of NPs in PBS solution (pH 7.4) at a concentration of 0.2 mg/mL was placed in an eppendorf vial and gently shaken in a Thermo Scientific Precision

Reciprocal Water Bath 25 at 37 ^{o}C or at 60 ^{o}C. At various times, the NP solution was centrifuged at a speed of 10000 rpm for 20 min, and 500 μl supernatant was collected for further HPLC analysis. The pellet was resuspended in fresh 1.0 mL PBS to preserve sink condition. All the release experiments lasted 8 hours. All samples under the same condition were duplicated at least. Cumulative DXM release, as measured by HPLC, was quantified with release time.

3.6 Characterization

3.6.1 ζ -Potential measurements

ζ –potential measurement is widely used for quantification of the electrical charge on colloids. It measures the potential difference between the charged surface of a dispersed particle and the medium. The absolute value of ζ –potential can be related the stability of colloids, where colloids with high ζ -potential are electrically stabilized while colloids with low ζ -potential tend to aggregate.[59] Here, the surface charge of bare DXM NPs and each adsorbing layer was characterized by ζ -potential measured with a Brookhaven ZetaPALS instrument. Each sample was run twice with each run consisting of 10 data points.

3.6.2 X-ray photoelectron spectroscopy

X-ray photoelectron spectroscopy (XPS) is a surface chemistry analysis technique that measures elemental composition and the chemical state of elements within the surface of materials. A beam of X-rays irradiates the surface. The kinetic

energy and number of electrons that escape from material are obtained and presented in XPS spectra. Here, a Kratos Axis Ultra Imaging X-ray photoelectron spectrometer was used to determine the surface elemental composition of each layer. The X-ray source was monochromatic aluminum (1486.6 eV). A 10 µl sample solution was dropped onto a piece of aluminum foil and dried overnight. Survey spectra were collected from 0 to 1200 eV with a pass energy of 160 eV.

3.6.3 Field-emission scanning electron microscopy

Images of bare DXM NPs were characterized by JEOL JSM-7500F field-emission scanning electron microscopy (FE-SEM). 10 µl NP solutions were diluted with isopropanol, filtered using an 0.8 µl filter, and drop cast onto a TEM copper grid. Samples were dried under ambient conditions, and stored in a vacuum oven at room temperature for 1 day before imaging. 4 nm of palladium/platinum was sputtered on the sample to minimize charging. The acceleration voltage was set to 3.0 kV.

3.6.4 Transmission electron microscopy

Images of 4.5 and 8.5 bilayers of PDAC/PSS LbL-coated DXM NPs were characterized by a JEOL 1200 EX Transmission Electron Microscopy (TEM). Both LbL shells were assembled from 0.5 M NaCl. A 2 µl LbL NPs solution was dropped on copper grid and dried at the room temperature. A CCD camera (SIA 15 C) was used for digital images. All images were acquired at 100 kV accelerating voltage.

3.6.5 High performance liquid chromatography

The concentration of DXM was assayed by high performance liquid chromatography (HPLC). HPLC uses high pressure to generate the flow that pass through a packed column. The components in a sample mixture being passed over the column are separated. Each component is identified and quantified using a detector. A reversed phase column was used in this study to separate components by polarity. A less polar molecule has more affinity to the filler material (silica) and thus elutes with a longer retention time. Each component appears as a peak in the chromatogram and its concentration can be quantified by integration of the area under each peak.

Here, the DXM concentration was assayed using a Thermo Scientific Dionex Ultimate 3000 UHPLC equipped with an Acclaim 120 C18 Reversed-Phase LC Column (250×4.6 mm, 5 μm). The supernatant was mixed with acetonitrile (1:1 v/v) and filtered by 0.2 μm filter. DXM absorbance was measured by a Diode Array Detector at 242 nm with a retention time of 3.3 min in 1mL/min 70/30 acetronitrile/water mobile phase. Column temperature was set to 30 ^{o}C and the sample temperature was maintained at 20 ^{o}C. Results were averaged from triplicate samples under the same condition. A calibration curve was obtained by plotting DXM integrated peak area versus DXM standard concentration.

4. RESULTS AND DISCUSSION

4.1 Introduction

In this chapter, LbL nanoshells encapsulating DXM NPs were fabricated. The successful deposition of a PDAC/PSS LbL coating onto DXM NPs was confirmed by ζ -potential, XPS, and TEM. The effect of varying (i) number of layers, (ii) ionic strength of the adsorption solutions, (iii) temperature, and (iv) outer-most layer on dexamethasone release *in vitro* is examined. Results indicate a thermo-responsive drug release from PDAC/PSS LbL nanoshells with tunable permeability by varying LbL assembly conditions.

4.2 The Size and Morphology of DXM NPs

Dexamethasone nanoparticles were fabricated by a two organic solvent evaporation technique described elsewhere.[55] Briefly, a solution of hydrophobic drug in acetone was emulsified with a second organic solvent of n-Heptane. Solid DXM particles of an average size of 201 ± 96 nm were formed (statistically obtained from different areas of SEM images). An FE-SEM image from a selected area is shown in Figure 4-1. The ζ -potential was -16 mV, which suggests that DXM NPs are negatively charged. The encapsulation efficiency determined by 3-1 was 35.3%.

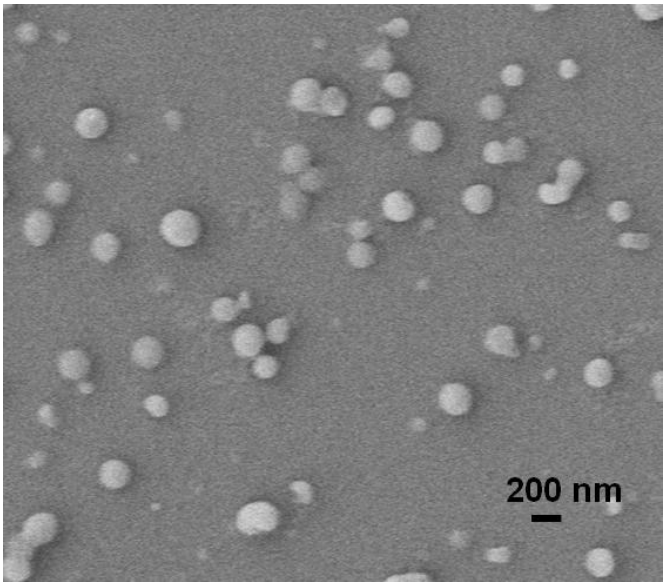

Figure 4-1. FE-SEM of bare DXM NPs. 4 nm of palladium/platinum was sputtered on the sample to minimize charging.

The modified solvent evaporation procedure described here relies on immiscible liquids to form droplets of drug which are hardened by solvent evaporation to form micro or nano particles.[58] Under low heat, acetone evaporates first, leaving DXM NPs suspended in n-Heptane. High-speed stirring continued to ensure the complete removal of n-Heptane. This modified solvent evaporation technique provides an efficient way to fabricate NPs. However, problems appear with the large distribution of particle size. Further optimization on emulsification speed, surfactant type/concentration, and organic to water volume ratio may be performed to control the size distribution of particles.[57]

4.3 Layer-by-Layer Assembly on DXM NPs

Layer-by-layer nanoshells were fabricated by assembling alternating layers of PDAC and PSS onto DXM NPs. Because each layer has its own characteristic elemental composition (PDAC has nitrogen and PSS has sulfur). X-ray photoelectron spectroscopy was used to analyze the surface composition of each deposited layer. From XPS survey scans in Figure 4-2, the binding energy at 168 eV representing for sulfur (S) 2p indicated deprotonated sulfonic acid. An increase in the S peak intensity corresponded to PSS layer adsorption and the intensity decreased after adding a layer of PDAC. The successful LbL coating on DXM NPs was also demonstrated by ζ -potential measurements, which characterize colloids surface charge and electrical stability (Figure 4-3).[60] A reversal in charge after each adsorbed layer and the high ζ –potential suggested that the polyelectrolytes were sequentially deposited.

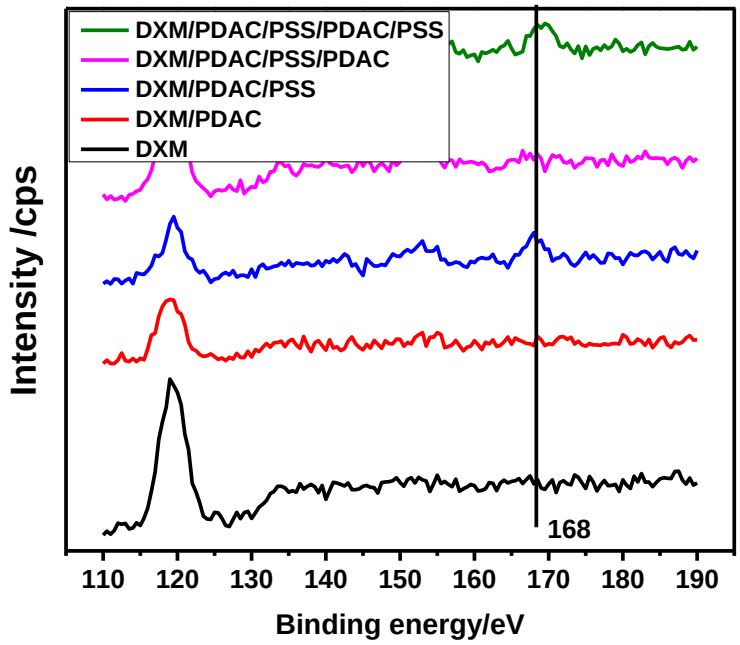

Figure 4-2. XPS survey scans spectra with pass energy 160 eV of DXM NPs encapsulated increasing number of layers of PDAC/PSS assembled at 0.5 M NaCl. The sulfur 2p peak at 168 eV confirmed the presence of PSS.

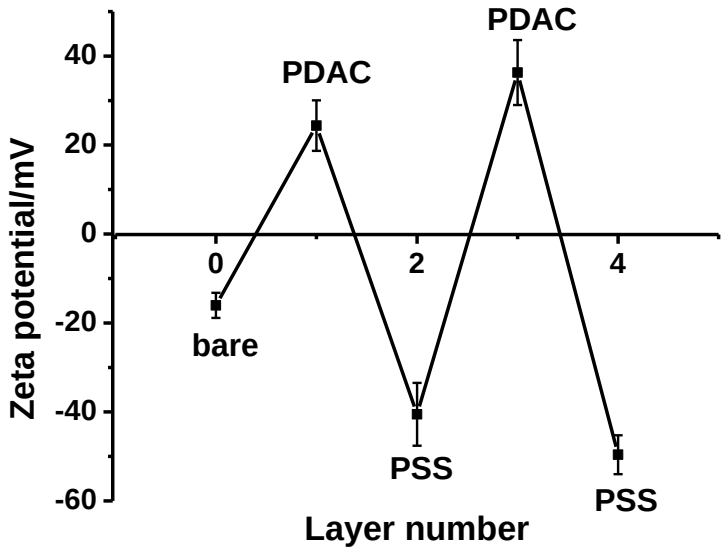

Figure 4-3. ζ –potential of two bilayers of PDAC/PSS LbL assemblies onto DXM NPs. The charge reversal after each layer deposited confirmed the successful LbL assembly on the DXM NP.

To visually examine the existence of the coating built on DXM NPs, TEM images of 4.5 and 8.5 bilayers of PDAC/PSS assembled at 0.5 M NaCl on DXM NPs are shown in Figure 4-4. The core appeared darker than the shell under TEM. This may be due to the difference in crystallinity of materials. DXM NPs are crystalline, while the layer is amorphous. At the magnification of 100,000, 4.5 bilayers were evident and the layer thickness was approximately 41.0 nm; 8.5 bilayers were evident and the layer thickness was approximately 72.1 nm.

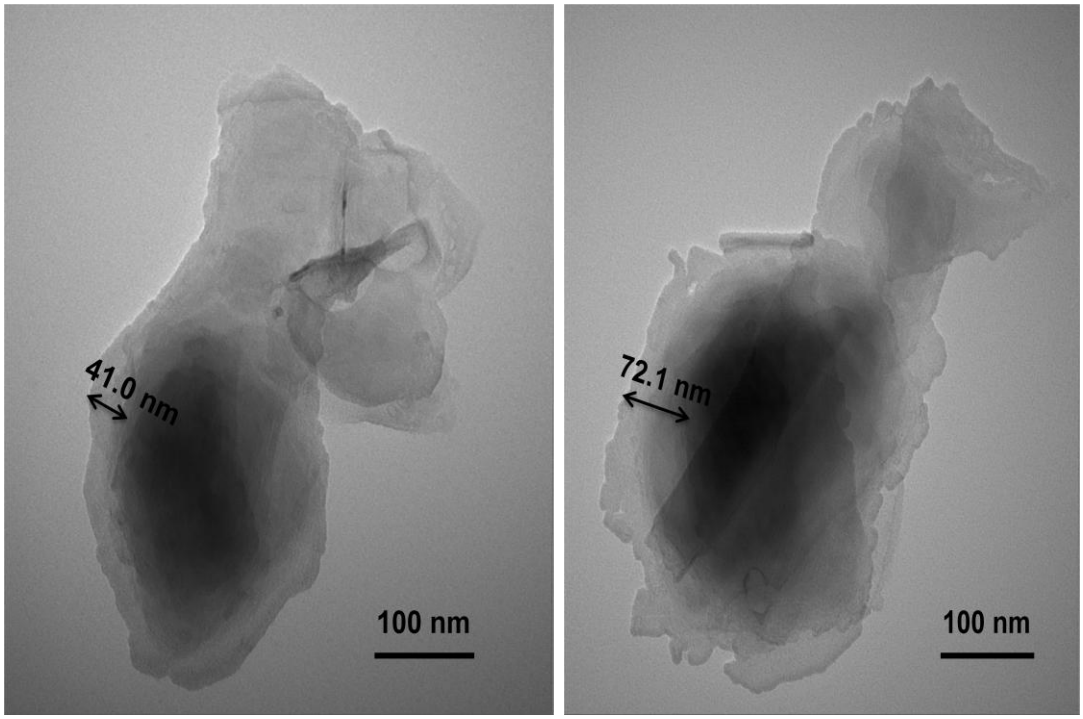

Figure 4-4. TEM of (left) $(PDAC/PSS)_{4.5}$, (right) $(PDAC/PSS)_{8.5}$ assembled at 0.5 M NaCl on DXM NPs at the magnification of 100,000.

4.4 *In Vitro* DXM Release from LbL Assemblies

In our *in vitro* release study, the cumulative DXM release from PDAC/PSS LbL-coated DXM NPs was investigated. The effect of varying (i) number of layers, (ii) ionic strength of the adsorption solutions, (iii) temperature, and (iv) outer-most layer on DXM release was examined.

4.3.1 Influence of number of layers on DXM release

a)

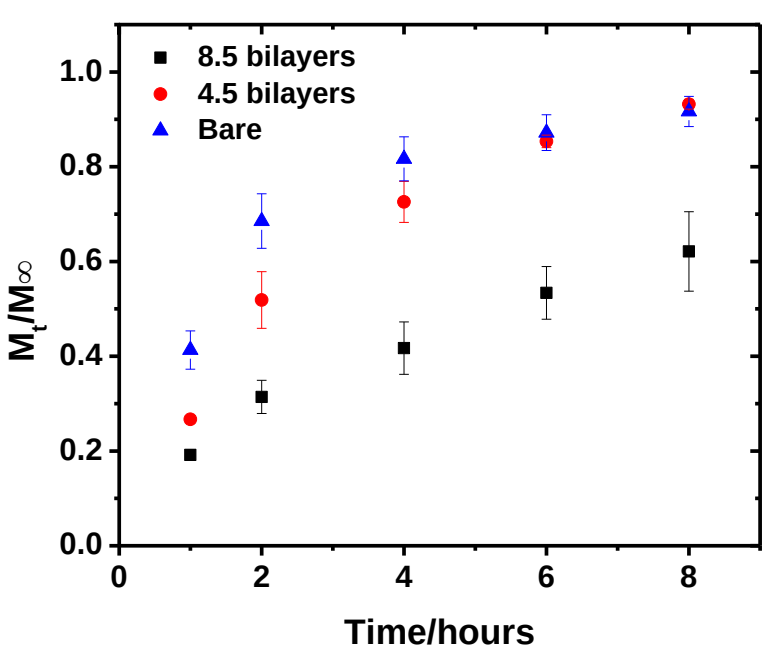

Figure 4-5. Cumulative DXM percentage release from a) Bare NPs (triangle) , $(PDAC/PSS)_{4.5}$ LbL-coated DXM NPs assembled at 0.5 M NaCl (square), and $(PDAC/PSS)_{8.5}$ LbL-coated DXM NPs assembled at 0.5M NaCl (circle), b) Bare NPs (triangle), $(PDAC/PSS)_{4.5}$ LbL-coated DXM NPs assembled without NaCl (square), and $(PDAC/PSS)_{8.5}$ LbL NPs assembled without NaCl (circle). Release experiments were carried out in PBS 7.4 at 37 ^{o}C. The Peppas model was applied to the release data from $(PDAC/PSS)_{4.5}$ LbL NPs assembled without NaCl (red shot dash) and $(PDAC/PSS)_{8.5}$ LbL NPs assembled without NaCl (black short dash), as discussed later.

b)

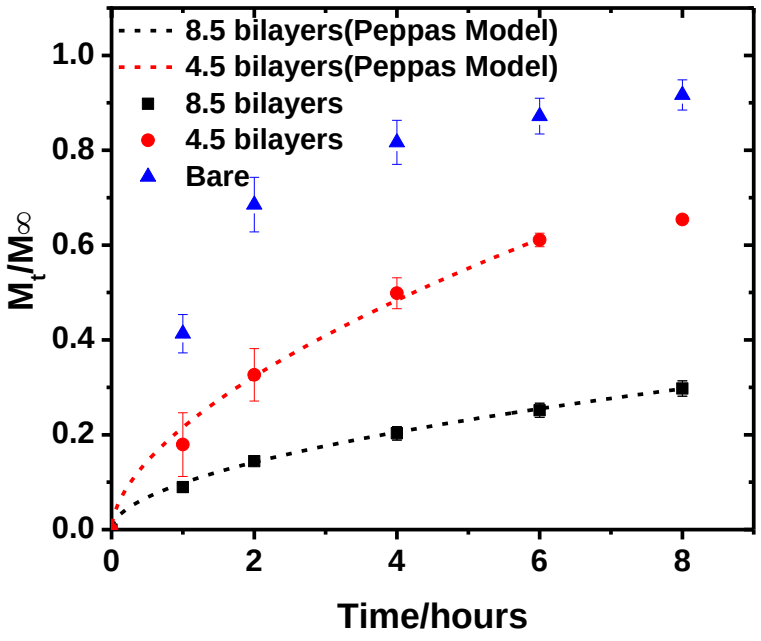

Figure 4-5 Continued.

Figure 4-5 a and 4-5 b display the DXM cumulative percentage release at 37 ^{o}C from bare NPs, $(PDAC/PSS)_{4.5}$ LbL-coated DXM NPs, and $(PDAC/PSS)_{8.5}$ LbL-coated DXM NPs. It was observed that bare NPs exhibited a burst release of 70% in 2 hours, while after encapsulating these NPs into various number of PDAC/PSS layers, this burst effect was eliminated. In this experiment, DXM NPs were encapsulated into PDAC/PSS LbL shells and then subjected to PBS that allowed for their controlled release. The existence of PDAC/PSS LbL nanoshells could increase the bioavailability of DXM and maintain a sustained release.

It has been established that the permeability of LbL nanoshells is strongly dependent on the thickness of LbL, which is controlled by varying the number of layers

within a range of a few nanometers.[61] From the results in Figure 4-5, for both ionic strengths explored, the release rate slowed down as number of layers increased. Within 8 hours, 65.3 ± 0.7% of DXM was released from $(PDAC/PSS)_{4.5}$ LbL-coated DXM NPs assembled without NaCl, whereas 30 ± 2% was released from $(PDAC/PSS)_{8.5}$ LbL-coated DXM NPs assembled without NaCl at 37 ^{o}C. For those LbL NPs assembled at 0.5 M NaCl, 93.2 ± 0.01% of DXM was released from $(PDAC/PSS)_{4.5}$ LbL NPs, while 62.5 ± 0.08% was released from $(PDAC/PSS)_{8.5}$ LbL-coated NPs. The trend suggests that the rate of DXM release from PDAC/PSS LbL nanoshells is a function of the thickness of shell. Similar trends were observed with paclitaxel NPs[62] and furosemide microcrystals[41] encapsulated within LbL shells.

With respect to film thickness, PDAC/PSS films assembled at 0.5 M NaCl grow exponentially, whereas PDAC/PSS films assembled without NaCl grow linearly. With equivalent number of layers, PDAC/PSS films assembled at 0.5 M NaCl are much thicker than films assembled without NaCl. However, the trends in Figure 4-6 have shown that the release rate was faster from exponentially growing LbL nanoshells. This is attributed to the "salt effect" and will be discussed in the subsequent section.

The internal structure of the LbL nanoshell, such as the size and concentration of free volume cavities, is known to have a critical effect on the transport of small molecules through the shell. We postulate that the mechanism responsible for the difference in DXM release from LbL NPs assembled at different conditions may be associated with the properties of free volume cavities within the LbL nanoshell. As suggested by Quinn *et al.*, for strong polyelectrolytes, the number of layers did not

change the free volume size but rather control the lateral gradient concentration, where there was more substrate compaction as the number of layers increased.[44] Hence, the trend observed here is not due to the variation of free volume properties.

The DXM release from PDAC/PSS LbL nanoshells with time appears to involve several stages that have been discussed before.[63, 64] As bulk solution diffuses into shell, drug NPs dissolution starts. When the concentration of DXM inside the shell reaches its saturation solubility, the concentration gradient between the interior and the bulk remains time-independent. The rate of drug release is then controlled by the permeability of LbL nanoshells. After the core is completely dissolved, the concentration of DXM decreases until an equilibrium concentration is achieved, resulting in the maximum release.

4.3.2 Influence of ionic strength on DXM release

Figure 4-6 a and 4-6 b display the DXM cumulative percentage release at 37 ^{o}C from LbL-coated DXM NPs assembled at 0.5 M NaCl and LbL-coated DXM NPs assembled without NaCl. The release rate became faster as ionic strength increased. For 8.5 bilayers LbL NPs, in 8 hours, $53 \pm 2\%$ of DXM was released from those assembled at 0.5 M NaCl, while $30 \pm 2\%$ was released from those assembled without NaCl. A similar trend was observed for 4.5 bilayers LbL-coated DXM NPs. Such behavior has been reported elsewhere[40] and is associated with the free defects in polyelectrolyte complex.

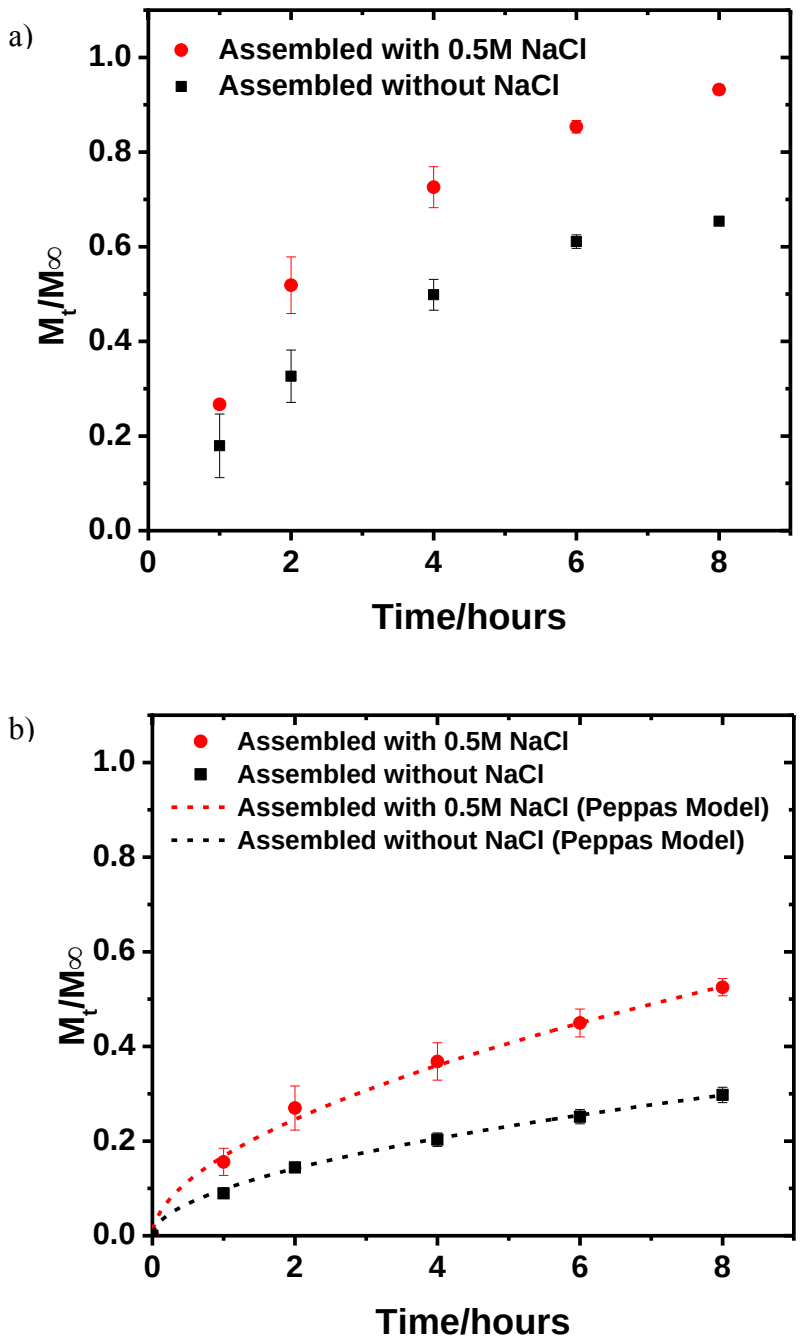

Figure 4-6. Cumulative DXM percentage release from a) $(PDAC/PSS)_{4.5}$ LbL-coated DXM NPs assembled at 0.5 M NaCl (circle) and without NaCl (square), b) $(PDAC/PSS)_{8.5}$ LbL-coated DXM NPs assembled at 0.5 M NaCl (circle) and without NaCl (square). Release experiments were carried out in PBS 7.4 at 37 ^{o}C. The Peppas model was applied to release data from $(PDAC/PSS)_{8.5}$ LbL-coated DXM NPs assembled at (red short dash) and without NaCl (black short dash).

The effect of ionic strength on the growth[7] and various properties of LbL assemblies has been widely discussed.[65, 66] At low ionic strength, LbL assemblies are elongated to form thin films, whereas at high ionic strength, they are in a coiled shape to form loops and tails. The difference in chain conformation is mainly due to a charge screening effect.[67] It has been suggested that the high ionic strength during the build up process favors polymer chain interdiffusion,[68] leading to a fuzzy structure. Recent studies further demonstrated that for strong polyelectrolytes, an increase in assembly salt concentration yielded the same free volume size but increased the free volume concentration.[44] Hence we postulate that the results observed in Figure 4-6 are likely attributed to the variation of free volume concentration, from many cavities at high ionic strength to a few cavities with similar size at low ionic strength.

It is interesting to note that the addition of salt in the release buffer is also known to enhance the permeability of LbL assemblies.[69] Added salt induces polyelectrolyte rearrangement and swells the LbL assembly, leading to polyelectrolyte binding site dissociation and new cavity formation.[67] It has been suggested that by exposing LbL assemblies to buffers with variable salt concentrations, the permeability of LbL obeys a power law $P \sim k[salt]^n$, where n is the ionic strength, k is proportionality constant and P is the permeability.[70] Such a phenomenon is suggested to be associated with the free energy of interpolyelectrolyte interaction, i.e. increasing the ionic strength of the surrounding solution decreases the free energy of polyelectrolyte interactions, causing an increase in permeability.[40] Changing the assembly and salt concentrations may induce nanopore formation. Caruso and co-workers introduced controlled nanometer-sized pores into

weak LbL assemblies by immersing them in pure water. Pores with 20-30 nm diameter size and 7-10 nm depth were formed in ten layers of PAH/PAA prepared from 0.2 M NaCl.[71] However, a significant increase in the ionic strength of the surrounding solution may cause dramatic weakening of polyelectrolyte interactions, which leads to LbL destabilization and decomposition.[37]

4.3.3 Influence of temperature on DXM release

The dissolution profiles of DXM bare NPs in PBS (pH 7.4) at 37 ^{o}C and 60 ^{o}C were shown in Figure 4-7. The dissolution rate was enhanced at 60 ^{o}C, as 78 $\pm$ 2% of DXM was released in 1 hour, as opposed to only 41 $\pm$ 4% of DXM was dissolved at 37 ^{o}C. This could be due to an increase in DXM solubility[72] or diffusion coefficient upon heating. According to Noyes–Whitney equation[73], an increase in saturation solubility or diffusion coefficient increases drug dissolution rate.

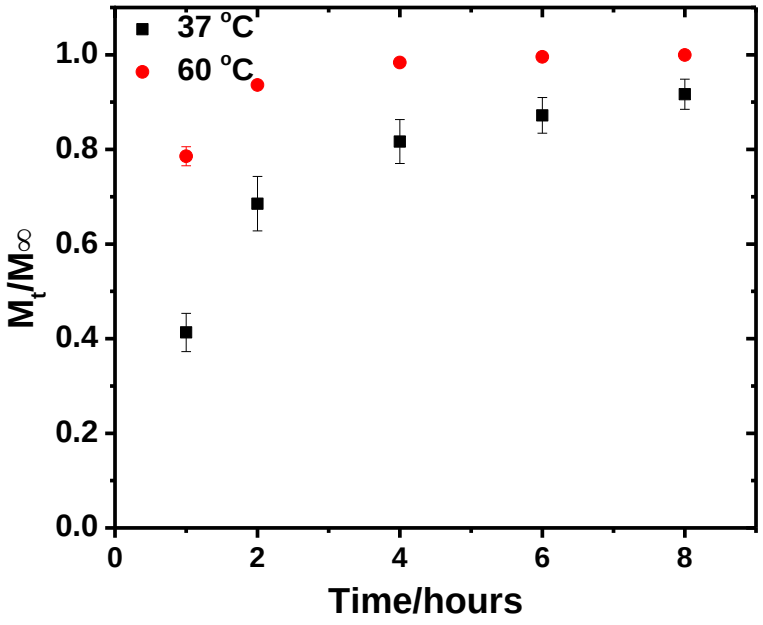

Figure 4-7. Cumulative DXM release from bare NPs at 37 °C (square) and 60 °C (circle) in PBS

To probe whether the glass transition at ~50 °C enhances the permeability of LbL nanoshells, the release of DXM from $(PDAC/PSS)_{4.5}$ and $(PDAC/PSS)_{8.5}$ LbL-coated DXM NPs assembled at 0.5 M NaCl at a temperature below and above the assemblies' T_g was investigated, Figure 4-8 a and 4-8 c. As a control, the release from LbL NPs assembled without NaCl was carried out under the same conditions since no glass transition was observed in those assemblies, Figure 4-8 b and 4-8 d. Generally, the release rate became faster as temperature increased. However, the change in release rate with respect to temperature was more extreme for LbL-coated DXM NPs exhibiting no glass transition. Within 8 hours, the cumulative DXM release from $(PDAC/PSS)_{8.5}$ LbL-coated DXM NPs assembled without NaCl increased by ~40%, whereas it increased by

23% for $(PDAC/PSS)_{4.5}$ LbL-coated DXM NPs assembled with 0.5 M NaCl. Although the absolute difference in the thermo-response of DXM release from LbL NPs varied from batch to batch, the overall trend was reproducible.

a)

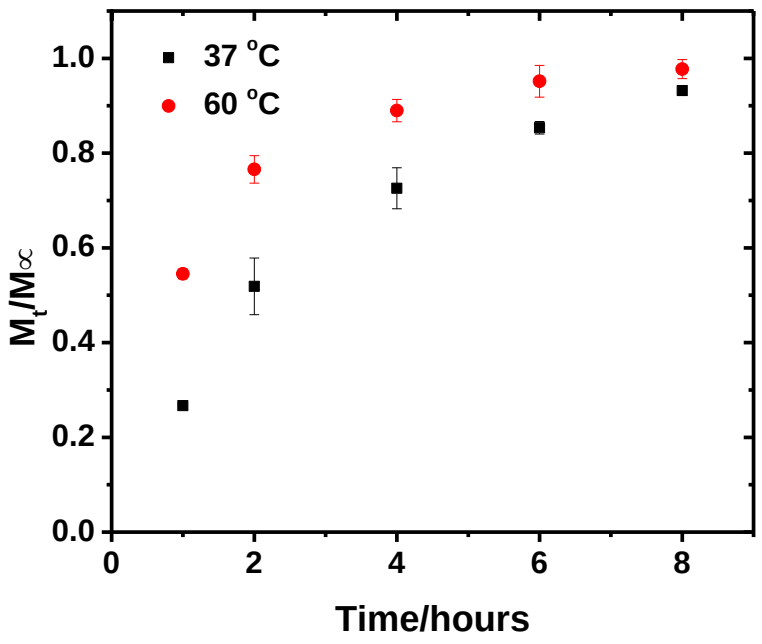

Figure 4-8. Thermo-response of a) $(PDAC/PSS)_{4.5}$ LbL-coated DXM NPs assembled at 0.5 M NaCl, b) $(PDAC/PSS)_{4.5}$ LbL-coated DXM NPs assembled without NaCl, c) $(PDAC/PSS)_{8.5}$ LbL-coated DXM NPs assembled at 0.5 M NaCl, d) $(PDAC/PSS)_{8.5}$ LbL-coated DXM NPs assembled without NaCl. The Peppas model was applied to release data for $(PDAC/PSS)_{8.5}$ LbL-coated DXM NPs at 60 ^{o}C(red short dash) and 37 ^{o}C (black short dash).

b)

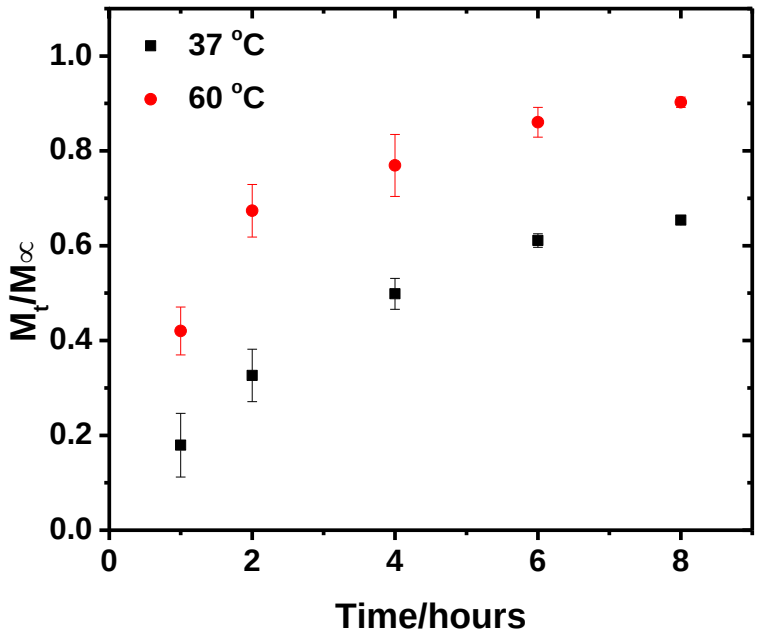

c)

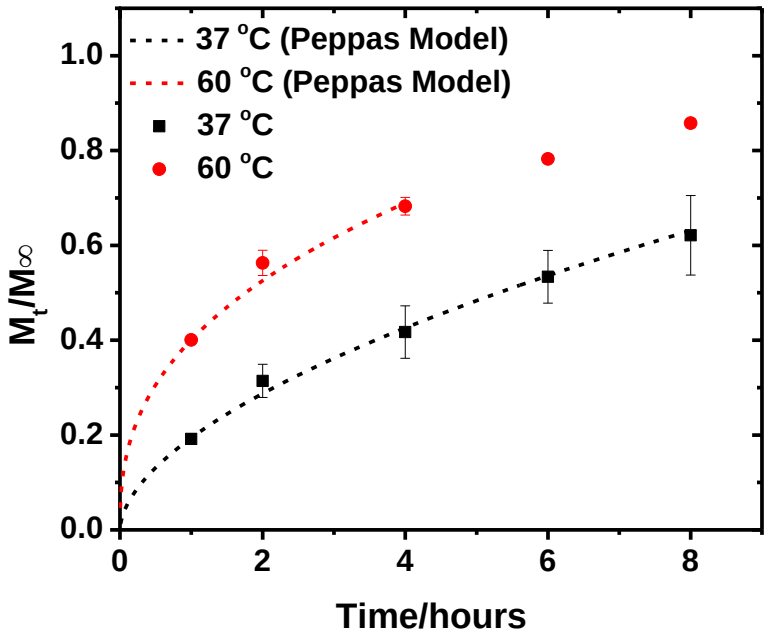

Figure 4-8 Continued

d)

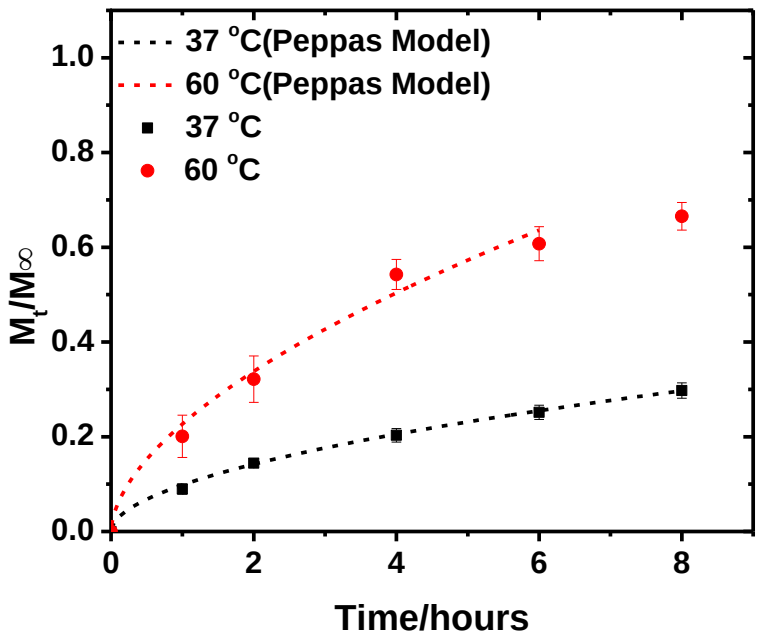

Figure 4-8 Continued

The experimental data shown in Figure 4-8 disproves the hypothesis that an increase in PDAC/PSS LbL shells mobility or viscoelasticity enhances DXM thermo-responsive release. It was expected that the DXM release from LbL NPs assembled at 0.5 M NaCl would experience more dramatic response to temperature than those assembled without NaCl. However, the results did not support this assumption. In diffusion-controlled drug release, the diffusion of DXM occurs through water-filled cavities and is associated with a dynamic activation process. Considering Cohen and Turnbull free volume theory,[74] the diffusing molecules, either DXM or water, resides temporally in a cavity and diffusion occurs when the solutes overcome a certain energy barrier and jump into the next cavity, or when two cavities meet each other and the solutes diffuse through one to another.[75] The diffusion coefficient may be related to an

average jump distance, the thermal velocity of solute, and the probability that there is a cavity adjacent to solute. At a given temperature, the rate of diffusion is determined by the probability of finding a sufficient free volume cavity for solute to pass through.[42] It was observed that a similar size but with a larger number of free volume cavity existed in strong layer pairs assembled at the higher salt concentration. This suggests a higher probability in PDAC/PSS LbL nanoshells having a free volume cavity when assembled at 0.5 M NaCl. As the temperature increases from 37 ^{o}C to 60 ^{o}C, there is a change in the film's overall viscoelasticity of PDAC/PSS LbL assembled at 0.5 M NaCl[14], allowing for polymer rearrangement and new cavity formation. However, there may be more change in probability of finding a free volume cavity of adequate size when using PDAC/PSS LbL assembled at 0.5 M NaCl, as compared to those assembled without NaCl, Figure 4-9.

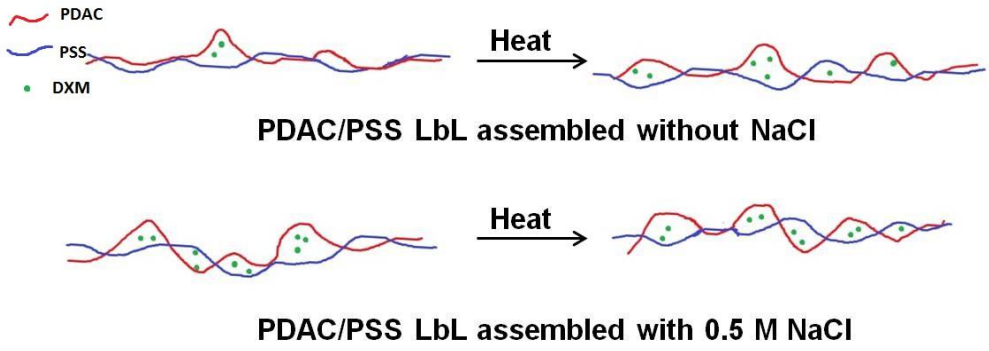

Figure 4-9. Hypothetical schematic illustrations of PDAC/PSS LbL assemblies rearranging upon heating.

4.3.4 Odd-even effect

Several groups have reported an "odd-even" effect for PDAC/PSS LbL capsules.[34, 76, 77] PSS-terminated capsules shrink upon heating, resulting in a denser sphere, whereas PDAC-terminated capsules swell. It was interesting for us to examine the DXM release from PSS-terminated LbL NPs at an elevated temperature. Figure 4-10 shows the thermo-response of DXM release from $(PDAC/PSS)_4$ LbL NPs assembled at 0.5 M NaCl. More thermo-response was observed as compared to Figure 4-8 a, where PDAC was the outer-most layer. At both 37 ^{o}C and 60 ^{o}C, the release rate became slower from PSS-terminated LbL NPs, as compared to the release rate from PDAC-terminated LbL NPs.

In this present work, an "odd-even" effect was observed for core-shell PDAC/PSS-DXM NPs. As suggested by Vidyasagar *et al.*,[14] upon heating, PSS-terminated LbL films became more rigid and the hydrated mass decreased. Köhler and co-workers[34,53, 78] also suggested that heating $(PDAC/PSS)_n$ microcapsules induced layers reorganization driven by two competing forces, i.e. the electrostatic forces and hydrophobic forces, which act outward and inward, respectively. Increasing temperature, for PSS-terminated capsules, tends to enhance hydrophobic interaction accompanied by a wall densification, whereas for PDAC-terminated capsules, such a tendency is overcompensated by the enhancement of electrostatic interactions resulting from the unbalanced ratio between polyelectrolytes. Köhler *et al.*[45] reported a decrease in apparent mesh size from 13 to 5 nm for PSS-terminated capsules after incubation at 50 ^{o}C. These values are attributed to the defects within LbL films.

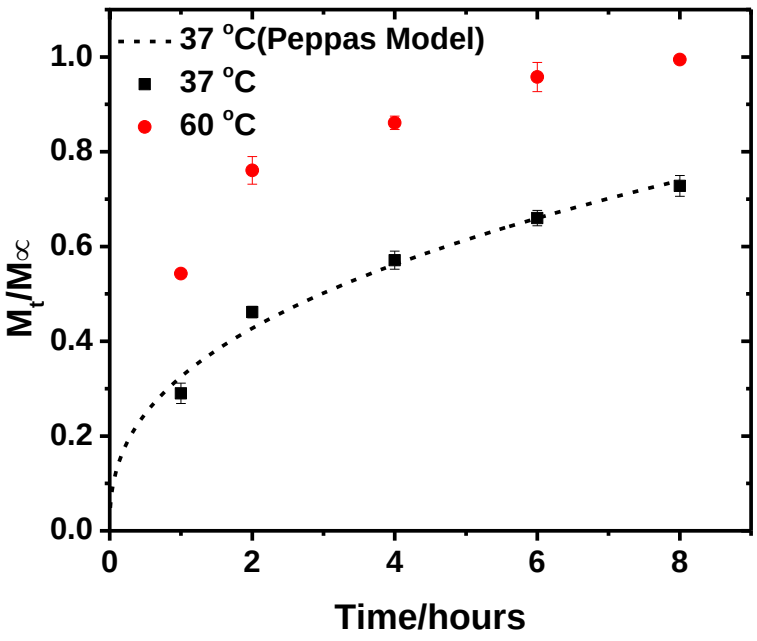

Figure 4-10. Cumulative DXM release from $(PDAC/PSS)_4$ LbL-coated DXM NPs assembled at 0.5 M NaCl at 37 °C(square) and 60 °C(circle).

4.3.5 Modeling of release kinetics

Higuchi model

To describe the DXM release rate from LbL NPs as the square root of time based on the principle of diffusion-controlled release, the Higuchi Model was applied,[79] Figure 4-11. The general form is:

$$M_t/M_\infty = k_H \times \sqrt{t}\ , \text{ with } k_H = \sqrt{2ADCs} \qquad 4\text{-}1$$

Where M_t is the cumulative absolute drug release amount at time t, M_∞ is the cumulative absolute drug release amount at infinite time, A is the drug mass per cubic centimeter in the matrix, D is the diffusional coefficient and C_s is the drug solubility.

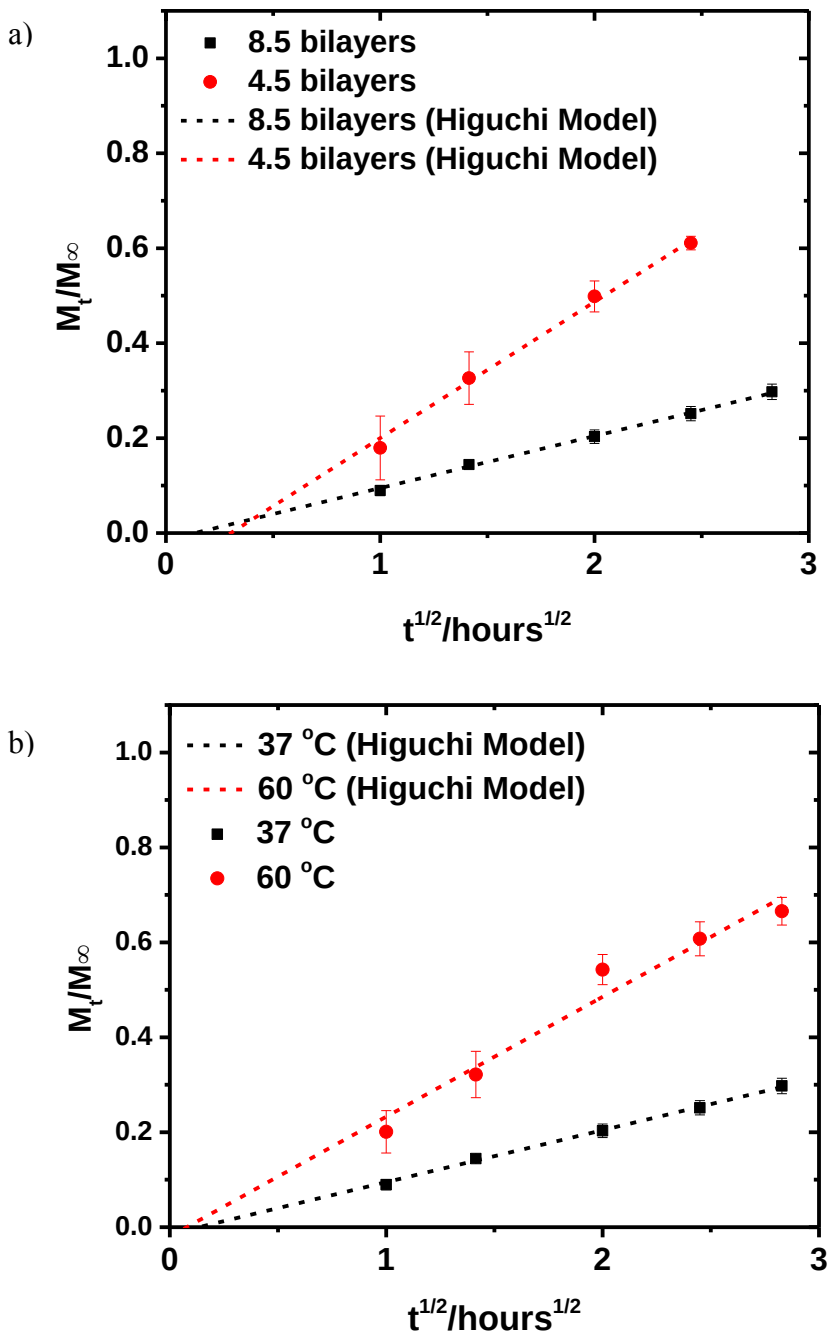

Figure 4-11. Higuchi model fitting exploring a) layer effect, b) salt effect, c) thermo-response of $(PDAC/PSS)_{8.5}$ LbL-coated DXM NPs assembled at 0.5 M NaCl, d) thermo-response of $(PDAC/PSS)_{8.5}$ LbL-coated DXM NPs assembled without NaCl. The slope (k), axis intercept (a) and correlation coefficient (R^2) were shown in Table 1.

c)

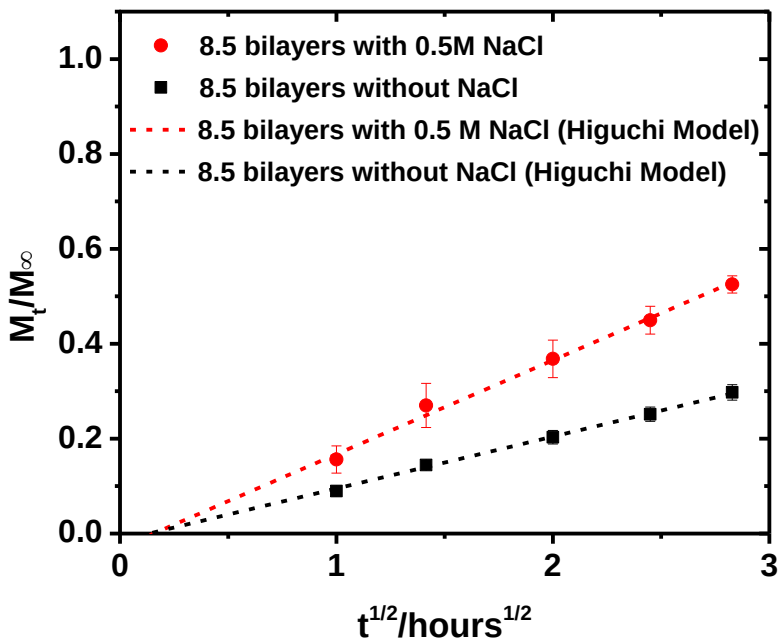

d)

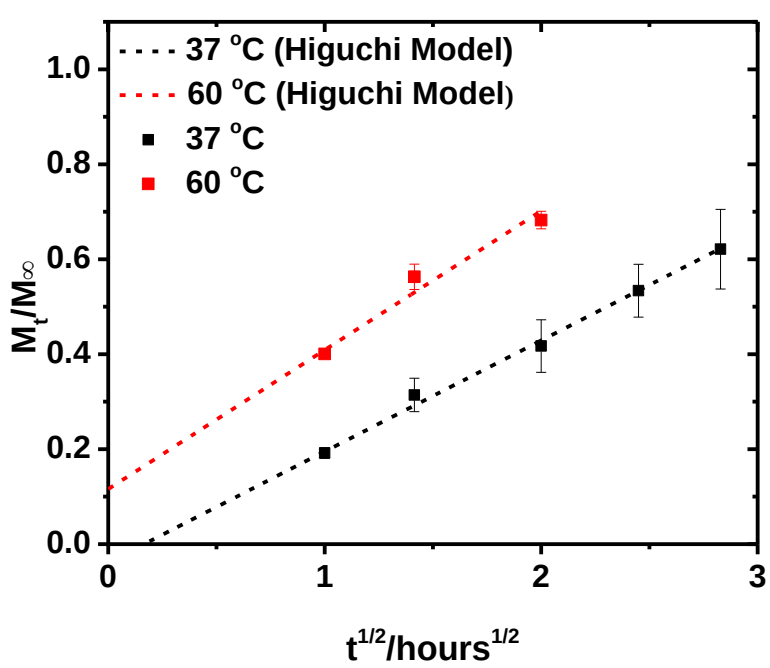

Figure 4-11 Continued

Plots from Higuchi model show good linearity for all release profiles explored, indicating that diffusion is likely to be the main factor controlling DXM release from those delivery systems. Release rate constants are obtained from the slope and correlation coefficients, Table 4-1. The Higuchi constant k_H is associated with the amount of drug per volume, diffusion coefficient, and drug solubility, and its value varied for different delivery systems. An increase in the number of layers appears to decrease the value of k_H. An increase in the ionic strength appears to increase the value of k_H. As temperature increased from 37 ^oC to 60 ^oC, the k_H of LbL-coated DXM NPs assembled at 0.5 M NaCl increased by 21%, whereas the k_H of LbL-coated DXM NPs assembled without NaCl increased by 127%.

Table 4-1. The Higuchi model fitting and release kinetics constants

Sample	Higuchi constant, $k_H^{-1/2}$	A	R^2	Figure reference
$(PDAC/PSS)_{4.5}$ assembled without NaCl, 37 ^oC	0.28 ± 0.01	-0.08 ± 0.03	0.99	Figure 4-11a
$(PDAC/PSS)_{8.5}$ assembled without NaCl, 37 ^oC	0.110 ± 0.004	-0.013 ± 0.007	0.99	Figure 4-11a, 4-11b, 4-11d
$(PDAC/PSS)_{8.5}$ assembled at 0.5 M NaCl, 37 ^oC	0.24 ± 0.01	-0.04 ± 0.01	0.99	Figure 4-11c
$(PDAC/PSS)_{8.5}$ assembled without NaCl, 60 ^oC	0.25 ± 0.03	-0.01 ± 0.07	0.93	Figure 4-11d
$(PDAC/PSS)_{8.5}$ assembled at 0.5M NaCl, 60 ^oC	0.29 ± 0.03	0.11 ± 0.03	0.98	Figure 4-11c

Korsmeyer–Peppas model (Power Law Equation)

The Korsmeyer–Peppas model,[80] or power law equation, $Mt/M_\infty=kt^n$, is a semi-empirical relation describing the general solute release behavior of controlled release systems. $(M_t)/(M_\infty)$ is the fractional drug release, t is the release time, k is a constant incorporating the coupling of solute diffusion and matrix relaxation phenomena, and n is the diffusional exponent, indicating the release mechanism. For release from a swellable sphere, solute release kinetics are dependent on drug diffusion and polymer relaxation. If the polymer swelling front advances faster than the drug diffusion, Fickian diffusion kinetics are expected and is defined by n=0.43. If drug diffusion is much faster than the swelling front advances, zero-order kinetics is expected and is defined by n=0.85.[81] In other words, higher n indicates that the release is more controlled by viscoelastic relaxation of the matrix, whereas lower n indicates that the release is more controlled by pure Fickian-diffusion. Many release behaviors fall between these limiting cases and is defined by n values between 0.43 and 0.85.[82] Because it is valid for the first 60% of the normalized drug release, we were able to fit the release profiles with at least four points (including fixed zero) lying within 60% of fractional release, Figure 4-5b, 4-6b, 4-8c, 4-8d, and 4-10. We obtained different values of exponent n and constant k as summarized in Table 4-2.

Table 4-2. The Korsmeyer–Peppas model fitting and possible mechanism of diffusional release from swellable controlled release systems

Sample	Diffusional exponent, n	Kinetic constant, k/h^{-n}	R^2	Release mechanism	Figure reference
Spherical sample	0.43	--	--	Fickian diffusion	--
	0.43<n<0.85			Anomalous(non-Fickian) transport	--
	0.85			Case-II transport	--
$(PDAC/PSS)_{4.5}$ assembled without NaCl, 37 °C	0.58 ± 0.05	0.22 ± 0.02	0.99	Non-Fickian diffusion	Figure 4-5b
$(PDAC/PSS)_{8.5}$ assembled without NaCl, 37 °C	0.53 ± 0.02	0.098 ± 0.003	0.99	Non-Fickian diffusion	Figure 4-5b, 4-6b, 4-8d
$(PDAC/PSS)_{8.5}$ assembled at 0.5 M NaCl, 37 °C	0.57 ± 0.02	0.194 ± 0.005	0.99	Non-Fickian diffusion	Figure 4-6b, 4-8c
$(PDAC/PSS)_{8.5}$ assembled without NaCl, 60 °C	0.6 ± 0.1	0.22 ± 0.04	0.94	Non-Fickian diffusion	Figure 4-8d
$(PDAC/PSS)_{8.5}$ assembled at 0.5 M NaCl, 60 °C	0.39 ± 0.03	0.400 ± 0.001	0.99	Fickian diffusion	Figure 4-8c
$(PDAC/PSS)_4$ assembled at 0.5 M NaCl, 37 °C	0.39 ± 0.04	0.32 ± 0.02	0.96	Fickian diffusion	Figure 4-10

The Korsmeyer–Peppas model fits the experimental data well with over 95% goodness of fit, enabling a further understanding of possible release mechanisms. Except

for the DXM release at 60 ^{o}C from $(PDAC/PSS)_{8.5}$ LbL nanoshells assembled at 0.5 M NaCl, the values of n are the same, lying between 0.43 and 0.85, indicating a non-Fickian or anomalous transport mechanism. For DXM release at 60 ^{o}C from $(PDAC/PSS)_{8.5}$ LbL-coated DXM NPs assembled at 0.5 M NaCl, the value 0.39 ± 0.03 of n indicates a Fickian transport mechanism. This result may not be reliable due to limited data points.

We next examined the influence of various parameters on kinetic constant k in the power law. An increase in the number of layers appears to decrease the value of k. An increase in the ionic strength appears to increase the value of k. For both $(PDAC/PSS)_{8.5}$ LbL NPs assembled at 0.5 M NaCl and without NaCl, k doubled as temperature increased.

In the power law, k has a specific physical significance $k=6(D/\pi a^2)^{1/2}$ in the case of Fickian-diffusion, where D is the diffusional coefficient and a denotes the radius of a sphere.[83] A decrease in k indicates either an increase in "a" or a decrease in D. As the number of layers increased, the films inner structure remained the same but thickness increased, suggesting an increase in "a". However, the influence on D was hard to conclude. Because PDAC/PSS LbL shell assembled without NaCl is much thinner compared to those assembled at 0.5 M NaCl,[14] as the ionic strength increased, "a" increased. The decrease in k should be associated with D. Upon heating, PDAC-terminated shells swell, resulting in an increase in "a". Thus the increase in k as temperature increased was attributed to an increase in D. The difference of temperature response is hard to be

correlated with either diffusional coefficient or particles radius because the degree of particles swollen upon heating for the respective ionic strength has not been investigated.

These new results allowed us to discuss the interplay of polymer chain mobility and free volume cavities affecting DXM release through PDAC/PSS LbL shells. Here, the rate of DXM release from exponentially growing LbL shells, which exhibits a glass transition, has more changes in polymer chain mobility. If polymer chains served to retard DXM movement through the assemblies, more changes in their mobility might cause more changes in the rate of DXM release. In contrast, the rate of DXM release from exponentially growing LbL shells saw less of a change upon heating, indicating that polymer chain mobility was not a dominant factor here. An increase in polymer chain mobility allows polymer rearrangement, which may lead to a change in the distribution of free volume cavities within the LbL. The difference of such a change in exponentially growing LbL shells and linearly growing LbL shells may explain the difference in the thermo-response of DXM release from these delivery systems. Thus it is interesting to next examine the properties of free volume cavities, including size and concentration, within exponentially growing LbL shells and linearly growing LbL shells at this present temperature window. A more clear explanation of how free volume cavities within LbL shells affect drug release will be discussed.

5. CONCLUSIONS

A thermo-responsive NP-based drug delivery system was developed using PDAC/PSS as the model. The influence of various parameters on DXM release from PDAC/PSS LbL NPs, such as number of layers, ionic strength of the adsorption solution, temperature and outer-most layer, has been investigated. Results disprove the hypothesis that the glass transition of PDAC/PSS LbL nanoshells enhances drug release in this particular DXM NPs-PDAC/PSS system.

DXM NPs at an average size of 201 $\pm$ 96 nm were obtained by a modified solvent evaporation technique and then encapsulated into strong polyelectrolytes of PDAC/PSS using a LbL assembly technique. The successful layer adsorption was demonstrated by ζ –potential, XPS and TEM. By applying the power law to DXM release profiles obtained, DXM release from LbL NPs was estimated to be non-Fickian diffusion. Results have shown a controlled DXM release rate from NPs by tuning number of layers and ionic strength of the adsorption solution. Results have also indicated a more temperature response in the rate of DXM release from linearly growing LbL of PDAC/PSS (assembled without NaCl), which do not exhibit a glass transition, than from exponentially growing LbL of PDAC/PSS (assembled at 0.5 M NaCl), which exhibit a glass transition. Such a difference was attributed to the variation in the change of free volume cavities existing in LbL, suggesting a possible approach to enhance thermo-responsive DXM release from LbL nanoshells by tailoring the properties of cavities. By tailoring the properties of cavities, an ideal thermo-responsive drug delivery

system may be obtained. This thermo-responsive NP-based drug delivery system with tunable permeability may possibly realize an “on” or “off” drug release mechanism in response to temperature, thus providing an alternative approach to delivering therapeutics with reduced toxic effects.

6. FUTURE WORK

Future work will investigate the change in the properties of free volume cavities within exponentially growing PDAC/PSS LbL shells and linearly growing PDAC/PSS LbL shells upon heating, thus elucidating more straightforward causes behind these thermo-responsive drug release phenomena. Characterization tools such as PAS can be used to measure the properties of free volume cavities. Other LbL systems that exhibit glass transition behavior will also be investigated on the properties of free volume cavities and thermo-responsive drug release. Considering factors affecting internal structure of LbL films, such as free volume cavities and polymer chain mobility, an ideal thermo-responsive drug delivery system may be obtained. Furthermore, *in vitro* release studies for investigated thermo-responsive delivery systems will be explored when exposed to an "on" or "off" drug release mechanism in response to heat.

The long term goal in this research is to develop a remotely triggered light-responsive drug delivery system. Near-infrared light (NIR) (650-900 nm) has become an attractive light resource because it is less harmful and allows for penetration of deep tissues. By inserting gold NPs into capsules wall, NIR-induced heat generation on gold NPs will raise the capsules' temperature, which may lead to an enhancement in drug permeability; therefore, remotely triggered NIR-responsive drug release can be achieved. Overall, the present research offers an opportunity in the development of the further combination of hyperthermia therapy with chemotherapy and photothermal therapy in cancer treatment.

REFERENCES

1 Vogelstein, B. and Kinzler, K. W. The Genetic Basis of Human Cancer. McGraw Hill Professional 2002.

2 Wang, C.; Xu, H.; Liang, C.; Liu, Y.; Li, Z.; Yang, G.; Cheng, L.; Li, Y., and Liu, Z. Iron Oxide @ Polypyrrole Nanoparticles as a Multifunctional Drug Carrier for Remotely Controlled Cancer Therapy with Synergistic Antitumor Effect. ACS NANO 2013, 7, 6782-6795.

3 Caruso, F. Generation of Complex Colloids by Polyelectrolyte-Assisted Electrostatic Self-Assembly. Aust. J. Chem. 2001, 54, 349-353.

4 Hammond, P. T. Building Biomedical Materials Layer-by-Layer. Materialstoday 2012, 15, 196-206.

5 del Mercato, L. L.; Rivera-Gil, P.; Abbasi, A. Z.; Ochs, M.; Ganas, C.; Zins, I.; Sönnichsen, C., and Parak, W. J. LbL Multilayer Capsules: Recent Progress and Future Outlook for Their Use in Life Sciences. Nanoscale 2010, 2, 458–467.

6 Becker, A. L.; Johnston, A. P. R., and Caruso, F. Layer-By-Layer-Assembled Capsules and Films for Therapeutic Delivery. Small 2010, 6, 1836–1852.

7 Guzmán, E.; Ritacco, H.; Rubio, J. E. F.; Rubio, R. G., and Ortega, F. Salt-induced Changes in the Growth of Polyelectrolyte Layers of Poly(diallyldimethylammonium chloride) and Poly(4-styrene sulfonate of sodium). Soft Matter 2009, 5, 2130–2142.

8 Wong, J. E,; Zastrow, H.; Jaeger, W., and von Klitzing, R. Specific Ion versus Electrostatic Effects on the Construction of Polyelectrolyte Multilayers. Langmuir 2009, 25, 14061-70.

9 Lee, D.; Nolte, A. J.; Kunz, A. L.; Rubner, M. F., and Cohen, R. E. PH-Induced Hysteretic Gating of Track-Etched Polycarbonate Membranes: Swelling/Deswelling Behavior of Polyelectrolyte Multilayers in Confined Geometry. J. Am. Chem. Soc.2006, 128, 8521–8529.

10 Shiratori, S. S. and Rubner, M. F. PH-Dependent Thickness Behavior of Sequentially Adsorbed Layers of Weak Polyelectrolytes. Macromolecules 2000, 33, 4213–4219.

11 Büscher, K.; Graf, K.; Ahrens, H., and Helm, C. A. Influence of Adsorption Conditions on the Structure of Polyelectrolyte Multilayers. Langmuir 2002, 18, 3585–3591.

12 Tan, H. L.; McMurdo, M. J.; Pan, G., and Gregory Van Patten, P. Temperature Dependence of Polyelectrolyte Multilayer Assembly. Langmuir 2003, 19, 9311–9314.

13 Gopinadhan, M.; Ahrens, H.; Günther, J-U. Approaching the Precipitation Temperature of the Deposition Solution and the Effects on the Internal Order of Polyelectrolyte Multilayers. Macromolecules 2005, 38, 5228–5235.

14 Vidyasagar A.; Sung, C.; Gamble, R., and Lutkenhaus, J. L. Thermal Transitions in Dry and Hydrated Layer-by-Layer Assemblies Exhibiting Linear and Exponential Growth. ACS NANO 2012, 6, 6174-6184.

15 Johansson, L. Diffusion and Interaction in Gels and Solutions. 2. Experimental Results on the Obstruction Effect. Macromolecules 1991, 24, 6019-6023.

16 Chandra, A.; Agrawal, R. C., and Mahipal, Y. K. Ion Transport Property Studies on PEO–PVP Blended Solid Polymer Electrolyte Membranes. J. Phys. D: Appl. Phys. 2009, 42, 135107.

17 Butler, G. B. and Angelo, R. J. Preparation and Polymerization of Unsaturated Quaternary Ammonium Compounds. VIII. A Proposed Alternating Intramolecular-Intermolecular Chain Propagation. J. Am. Chem. Soc. 1957, 79, 3128.

18 Jaber J. A., Schlenoff J. B. Mechanical Properties of Reversibly Cross-Linked Ultrathin Polyelectrolyte Complexes. J. Am. Chem. Soc. 2006, 128, 2940.

19 Provan D, Stasi R, Newland A. C., Blanchette V. S., Bolton-Maggs P, Bussel J. B., Chong B. H., Cines D. B., Gernsheimer T. B., Godeau B, Grainger J, Greer I, Hunt B. J., Imbach P. A., Lyons G, McMillan R, Rodeghiero F, Sanz M. A., Tarantino M, Watson S, Young J, Kuter D. J. International consensus report on the investigation and management of primary immune thrombocytopenia. Blood 2010, 115, 168–86.

20 Hickey, T.; Kreutzer, D.; Burgess, D. J., and Moussy, F. Dexamethasone/PLGA microspheres for continuous delivery of an anti-inflammatory drug for implantable medical devices. Biomaterials 2002, 23, 1649-1656.

21 Zhong, Y.; McConnell, G. C.; Ross, J. D.; DeWeerth, S. P., and Bellamkonda, R. V. A Novel Dexamethasone-releasing, Anti-inflammatory Coating for Neutral Implants. Proceedings of the 2 International IEEE EMBS Conference on Neural Engineering, Arlington, Virginia, March 16 - 19, 2005.

22 Kim D. H. and Martin, D. C. Sustained Release of Dexamethasone from Hydrophilic Matrices using PLGA Nanoparticles for Neutral Drug Delivery. Biomaterials 2006, 3031-3037.

23 Allen, T. M. and Cullis P. R. Drug Delivery Systems: Entering the Mainstream. Science 2004, 303, 1818-1822.

24 Kolishetti, N.; Dhar S.; Valencia P. M.; Lin L. Q.; Karnik R.; Lippard S. J.; Langer R.; and Farokhzad O. C. Engineering of Self-Assembled Nanoparticle Platform for Precisely Controlled Combination Drug Therapy. PNAS 2010, 107, 17939–17944.

25 Langer R. Drug Delivery and Targeting. Nature 1998, 392, 5–10.

26 Desai N. Challenges in Development of Nanoparticle-Based Therapeutics. AAPS 2012, 14, 282-295.

27 Brigger, I.; Dubernet, C.; Couvreur, P. Nanoparticles in Cancer Therapy and Diagnosis. Adv Drug Deliv Rev. 2002, 54, 631-51.

28 Parveen, S.; Misra, R., and Sahoo, S. K. Nanoparticles: A Boon to Drug Delivery, Therapeutics, Diagnostics and Imaging. Nanomedicine: Nanotechnology, Biology, and Medicine 2012, 8, 147–166.

29 Yoo, J. W.; Doshi, N. and Mitragotri, S. Adaptive Micro and Nanoparticles: Temporal Control over Carrier Properties to Facilitate Drug Delivery. Adv Drug Deliv Rev. 2011, 63, 1247–1256.

30Decher G. Fuzzy Nanoassemblies: Toward Layered Polymeric Multicomposites. Science 1997, 277, 1232-1233.

31 Ibarz, G.; Dähne, L.; Edwin Donath, E., and Möhwald, H. Smart Micro- and Nanocontainers for Storage, Transport, and Release. Adv. Mater. 2001, 13, 1324–1327.

32 Zhu, Z. and Sukhishvili, S. A. Temperature-Induced Swelling and Small Molecule Release with Hydrogen-Bonded Multilayers of Block Copolymer Micelles. ACS NANO 2009, 3, 3593-3605.

33 Kharlampieva, E.; Kozlovskaya, V.; Tyutina, J. and Sukhishvili, S. A. Hydrogen-Bonded Multilayers of Thermoresponsive Polymers. Macromolecules 2005, 38, 10523-10531.

34 Bédard, M. F.; Braun, D.; Sukhorukov, G. B. and Skirtach, A. G. Toward Self-Assembly of Nanoparticles on Polymeric Microshells: Near-IR Release and Permeability. ACS NANO 2008, 2, 1807-1816.

35 Kozlovskaya, V.; Kharlampieva, E.; Drachuk, I.; Cheng, D., and Tsukruk, V. V. Responsive Microcapsule Reactors Based on Hydrogen-Bonded Tannic Acid Layer-by-Layer Assemblies. Soft Matter 2010, 6, 3596-3608.

36 Delcea, M.; Möhwald, H.; Skirtach, A. G. Stimuli-responsive LbL capsules and nanoshells for drug delivery. Adv Drug Deliv Rev. 2011, 63, 730–747.

37 Mansouri, S.; Winnik, F. M., and Tabrizian, M. Modulating the Release Kinetics through the Control of the Permeability of the layer-by-Layer Assembly: a Review. Expert Opin. Drug Deliv. 2009, 6,585-597.

38 Qiu, X.; Leporatti, S.; Donath, E., and Möhwald, H. Studies on the Drug Release Properties of Polysaccharide Multilayers Encapsulated Ibuprofen Microparticles. Langmuir 2001, 17, 5375-5380.

39 Angelatos, A. S.; Johnston, A. P. R.; Wang, Y., and Caruso, F. Probing the Permeability of Polyelectrolyte Multilayer Capsules via a Molecular Beacon Approach. Langmuir 2007, 23, 4554-4562.

40 Antipov, A. A.; Gleb B. Sukhorukov, G. B., and Möhwald, H. Influence of the Ionic Strength on the Polyelectrolyte Multilayers' Permeability. Langmuir 2003, 19, 2444-2448.

41 Antipov, A. A.; Gleb B. Sukhorukov, G. B.; Donath, E., and Möhwald, H. Sustained Release Properties of Polyelectrolyte Multilayer Capsules. J. Phys. Chem. B 2001, 105, 2281-2284.

42 Amsden, B. Solute Diffusion within Hydrogels. Mechanism and Models. Macromolecules 1998, 31, 8382-8395.

43 Chávez, F. V. and Schönhof, M. Pore Size Distributions in Polyelectrolyte Multilayers Determined by Nuclear Magnetic Resonance Cryoporometry. The Journal of Chemical Physics 2007, 126, 104705.

44 Quinn, J. F.; Pas, S. J.; Quinn, A.; Yap, H. P.; Suzuki, R.; Tuomisto, F.; Shekibi, B. S.; Mardel, J. I.; Hill, A. J., and Caruso, F. Tailoring the Chain Packing in Ultrathin Polyelectrolyte Films Formed by Sequential Adsorption: Nanoscale Probing by Positron Annihilation Spectroscopy. J. Am. Chem. Soc. 2012, 134, 19808-19819.

45 Köhler, K. and Sukhorukov, G. B. Heat Treatment of Polyelectrolyte Multilayer Capsules: A Versatile Method for Encapsulation. Adv. Funct. Mater. 2007, 17, 2053–2061.

46 Quinn, J. F. and Caruso, F. Facile Tailoring of Film Morphology and Release Properties Using Layer-by-Layer Assembly of Thermoresponsive Materials. Langmuir 2004, 20, 20-22.

47 Tan, W. S.; Cohen, R. E.; Rubner, M. F., and Sukhishvili S. A. Temperature-Induced, Reversible Swelling Transitions in Multilayers of a Cationic Triblock Copolymer and a Polyacid. Macromolecules 2010, 43, 1950–1957.

48 Wang, A.; Tao, C.; Cui, Y.; Duan, L.; Yang, Y.; Li, J. Assembly of Environmental Sensitive Microcapsules of PNIPAAm and Alginate Acid and Their Application in Drug Release. Journal of Colloid and Interface Science 2009, 332,271–279.

49 Sukhishvili, S. A. Responsive Polymer Films and Capsules via Layer-by-Layer Assembly. Current Opinion in Colloid & Interface Science 2005, 10, 37 – 44.

50 Jaber, J. A. and Schlenoff, J. B. Polyelectrolyte Multilayers with Reversible Thermal Responsivity. Macromolecules 2005, 38, 1300-1306.

51 Lin, C. Y.; Liao, K. H.; Su, C. F.; Kuo, C. H. and Hsieh, K. H. Smart Temperature-Controlled Water Vapor Permeable Polyurethane Film. Journal of Membrane Science 2007, 299, 91–96.

52 Renate Mueller, R.; Köhler, K.; Weinkamer, R.; Sukhorukov, G. B., and Fery, A. Melting of PDAC/PSS Capsules Investigated with AFM Force Spectroscopy. Macromolecules 2005, 38, 9766-9771.

53 Köhler, K.; Möhwald, H., and Sukhorukov, G. B. Thermal Behavior of Polyelectrolyte Multilayer Microcapsules: 2. Insight into Molecular Mechanisms for the PDADMAC/PSS System. J. Phys. Chem. B 2006, 110, 24002-24010.

54 Ghostine, R. A. and Schlenoff, J. B. Ion Diffusion Coefficients Through Polyelectrolyte Multilayers: Temperature and Charge Dependence. Langmuir 2011, 27, 8241–8247.

55 Alisar S. Zahr, A. S.; de Villiers, M., and Pishko, M. V. Encapsulation of Drug Nanoparticles in Self-Assembled Macromolecular Nanoshells. Langmuir 2005, 21, 403-410.

56 Li, M.; Rouaud, O. and Poncelet, Denis. Microencapsulation by Solvent Evaporation: State of the Art for Process Engineering Approaches. International Journal of Pharmaceutics 2008, 363, 26–39.

57 Watts, P. J.; Davies, M. C., and Melia, C. D. Microencapsulation using Emulsion Solvent Evaporation-An Overview of Techniques and Applications. Critical Reviews in Therapeutics Drug Carrier Systems 1990, 7, 235-259.

58 Yeh, M. K.; Coombes, A. G. A.; Jenkins, P. G., and Davis, S. S. A Novel Emulsification-Solvent Extraction Technique for Protein Loaded Biodegradable Microparticles for Vaccine Drug Delivery. Journal of Controlled Release 1995, 33, 437-445.

59 Greenwood, R. and Kendall, K. Selection of Suitable Dispersants for Aqueous Suspensions of Zirconia and Titania Powders using Acoustophoresis Journal of the European Ceramic Society 1999, 19, 479–488.

60 Coombes, A.G.A.; Tasker, S.; Lindblad, M.; Holmgre, J.; Hoste, K.; Toncheva, V.; Schacht, E.; Davies, M. C.; Illum, L., and Davis, S. S. Biodegradable Polymeric Microparticles for Drug Delivery and Vaccine Formulation: the Surfade Attachment of

Hydrophilic Species using the Concept of Poly(ethylene glycol) Anchoring Segments. Biomaterials 1997, 18, 1153-1161.

61 Dong, W. F.; Ferri, J. K.; Adalsteinsson, T.; Schönhoff, M.; Sukhorukov, G. B., and Möhwald, H. Influence of Shell Structure on Stability, Integrity and Mesh Size of Polyelectrolyte Capsules: Mechanism and Strategy for Improved Preparation. Chem. Mater. 2005, 17, 2603-2611.

62 Yu, X. and Pishko, M. V. Nanoparticle-Based Biocompatible and Targeted Drug Delivery: Characterization and in Vitro Studies. Biomacromolecules 2011, 12, 3205–3212.

63 Shi, X. and Caruso, F. Release Behavior of Thin-Walled Microcapsules Composed of Polyelectrolyte Multilayers. Langmuir 2001, 17, 2036-2042.

64 Qiu, X.; Leporatti, S.; Donath, E. and Möhwald, H. Studies on the Drug Release Properties of Polysaccharide Multilayers Encapsulated Ibuprofen Microparticles. Langmuir 2001, 17, 5375-5380.

65 McAlney, R. A.; Dudnik, V., and Goh, M. C. Kinetics of Salt-Induced Annealing of a Polyelectrolyte Multilayer Film Morphology. Langmuir 2003, 19, 3947-3952.

66 Han, L.; Mao, Z.; Wuliyasu, H.; Wu, J.; Gong, X.; Yang, Y., and Gao, C. Modulating the Structure and Properties of Poly(sodium 4-styrenesulfonate)/Poly(diallyldimethylammonium chloride) Multilayers with Concentrated Salt Solutions. Langmuir 2012, 28, 193–199.

67 Ladam, G.; Schaad, P.; Veogel, J. C.; Schaaf, P.; Decher, G., and Cuisinier, F. In Situ Determination of the Structural Properties on Initially Deposited Polyelectrolyte Multilayers. Langmuir 2000, 16, 1249-1255.

68 Picar, L.; Mutterer, J.; Richer, L.; Luo, Y.; Prestwich, G. D.; Schaaf, P.; Veogel, J.-C. and Lavalle, P. Molecular Basis for the Explanation of the Exponential Growth of Polyelectrolyte Multilayers. PNAS 2002, 99, 12531-12535.

69 Lu H and Hu N. Salt-induced Swelling and Electrochemical Property Change of Hyaluronic Acid/Myoglobin Multilayer Films. J Phys Chem B 2007, 111, 1984-93.

70 Farhat, T. R. and Schlenoff J. B. Ion Transport and Equilibria in Polyelectrolyte multilayers. Langmuir 2001, 17, 1184-1192.

71 Fery, A.; Schöler, B.; Cassagneau, T. and Caruso, F. Nanoporous Thin Films Formed by Salt-Induced Structural Changes in Multilayers of Poly(acrylic acid) and Poly(allylamine). Langmuir 2001, 17, 3779-3783.

72 Chim, R.; Marceneiro S.; de Matos, M. B. C.; Braga, M. E. M.; Dias, A. M. A., and de Sousa, H. C. Solubility of Poorly Soluble Drugs in Supercritical Carbondioxide: Experimental Measurement and Density-Based Correlations. III Iberoamerican Conference on Supercritical Fluids Cartagena de Indias (Colombia), 2013.

73Kocbek, P.; Baumgartner, S.; Kristl, J. Preparation and Evaluation of Nanosuspensions for Enhancing the Dissoution of Poorly Soluble Drugs. International Journal of Pharmaceutics 2006, 312, 179-186.

74 Cohen, M. H. Molecular Transport in Liquids and Glasses. The Journal of Chemical Physics 1959, 31, 1164-1169.

75 Petit, J.-M.; Roux, B., and Zhu, X. X. A New Physical Model for the Diffusion of Solvents and Solute Probes in Polymer Solutions. Macromolecules 1996, 29, 6031-6036.

76 Köhler, K.; Shchukin, D. G.; Möhwald, H., and Sukhorukov, G. B. Thermal Behavior of Polyelectrolyte Multilayer Microcapsules. 1. The Effect of Odd and Even Layer Number. J. Phys. Chem. B 2005, 109, 18250-18259.

77 Köhler, K.; Biesheuvel, P. M.; Weinkamer, R.; Möhwald, H., and Sukhorukov, G. B. Salt-induced Swelling to Shrinking Transition in Polyelectrolyte Multilayer Capsules. Physical Review Letters 2006, 97, 188301.

78 Köhler, K.; Shchukin, D. G.; Möhwald, H. and Sukhorukov, G. B. Thermal Behavior of Polyelectrolyte Multilayer Microcapsules. 1. The Effect of Odd and Even Layer Number. J. Phys. Chem. B 2005, 109, 18250-18259.

79 Higuchi, T. Rate of Release of Medicaments from Ointment Bases Containing Drugs in Suspension. Journal of Pharmaceutical Sciences 1961, 50, 874-875.

80 Ritger, P. L. and Peppas, N. A. A Simple Equation for Decription of Solute Release II: Fickian and Anomalous Release from Swellable Devices. Journal of Controlled Release 1987, 5, 37-42.

81 Lee, P. I. Kinetics of Drug Release from Hydrogel Matrices. Journal of Controlled Release 1985, 2, 277-288.

82 Siepmann J. and Peppas N. A. Higuchi equation: Derivation, Applications, Use and Misuse. International Journal of Pharmaceutics 2011, 418, 6–12.

83 Ritger, P. L. and Peppas, N. A. A Simple Equation for Description of Solute Release I. Fickian and Non-fickian Release from Non-Swellable Devices in the Form of Slabs, Spheres, Cylinders or Discs. Journal of Controlled Release 1987, 5, 23-26.